2 Results

2.1 Specificity ELISA

Common and different properties of four mouse monoclonal antibodies, which all recognise the Lewis Y carbohydrate epitope, were analysed by screening them using enzyme linked immunosorbent assay (ELISA) technique. The antibodies were generated some years ago by Uwe Karsten at the MDC Berlin. 86 different carbohydrate polyacrylamide (PAA) conjugates were used to identify the fine specificity of the four different clones, which are named A51-B/A6 (IgA, κ), A46-B/B10 (IgM, κ), A70-C/C8 (IgM, κ), and A70-A/A9 (IgG1, κ). The carbohydrate-PAA conjugates were coated on microtiter plates, the individual supernatants were added and an anti-mouse Ig peroxidase coupled (POD) antibody was used for detection. As a result carbohydrate specificities of the individual antibodies are determined.

Figure 7 A shows a strong signal for A51-B/A6 binding to Lewis Y, H type 2, and the H disaccharide. In addition a very small signal towards Globo H was also found. Interpretation of the experimental results reveals a fine specificity of A51-B/A6 for the H disaccharide either alone or attached on a type 2 chain.

The antibody A46-B/B10 recognised H type 2 and Lewis Y strongly in ELISA (Figure 7 B). This proposes the H type 2 as the epitope. The additional fucose in Lewis Y does not obstruct the recognition of the H type 2.

For A70-C/C8 exclusive binding to Lewis Y was found. Figure 8 A shows that none of the other investigated carbohydrates show any binding.

Figure 8 B shows Lewis Y, Lewis b and Globo H as the interacting partners for A70-A/A9 in the carbohydrate ELISA. For this antibody a trace signal was also observed against H type 2. The H disaccharide carbohydrate structure is present in all compounds, though the picture is complicated by strong binding to Lewis Y and Lewis b as well as weak and no binding to H type 2 and H type 1, respectively.

The specificity ELISAs identified a small group of related carbohydrates to be the antigen for these four antibodies, namely H disaccharide, H type 2, Lewis Y, Lewis b, and Globo H. A further testing of the binding of the antibodies in ELISA with use of a very high concentration of antibody (50µg/ml) was made to these antigens to identify low binding too (data not shown). One deviation from the above described binding patterns was found, A46-B/B10 was able to bind to the H disaccharide at this concentration.

Figure 9 shows the titration of the supernatants on the immobilised antigens in ELISA. All antibodies showed concentration dependent binding of the tested antigens. In our hands the average antibody concentration in the supernatants of mouse monoclonal IgG antibodies is 20µg/ml, of IgAs 15µg/ml, and of IgMs 5µg/ml. A51-B/A6 binding to Lewis Y and H type 2 showed the same concentration dependency, whereas a slightly lower signal was observed for the H disaccharide. This indicates that the full epitope involves some part of the GlcNAc carbohydrate, though signal intensity not necessarily correlates to affinity. For A46-B/B10 the concentration dependency of Lewis Y also coincides with the H type 2. A70-A/A9 reached a signal of 1.2 against Lewis Y, which does not change in the first dilutions. This indicates that the signal is at maximum at a 40 times dilution. In contrast to this it was not possible to reach the same maximum against Lewis b when diluted supernatant was used. The ELISA clearly revealed that the binding to Lewis b is weaker.

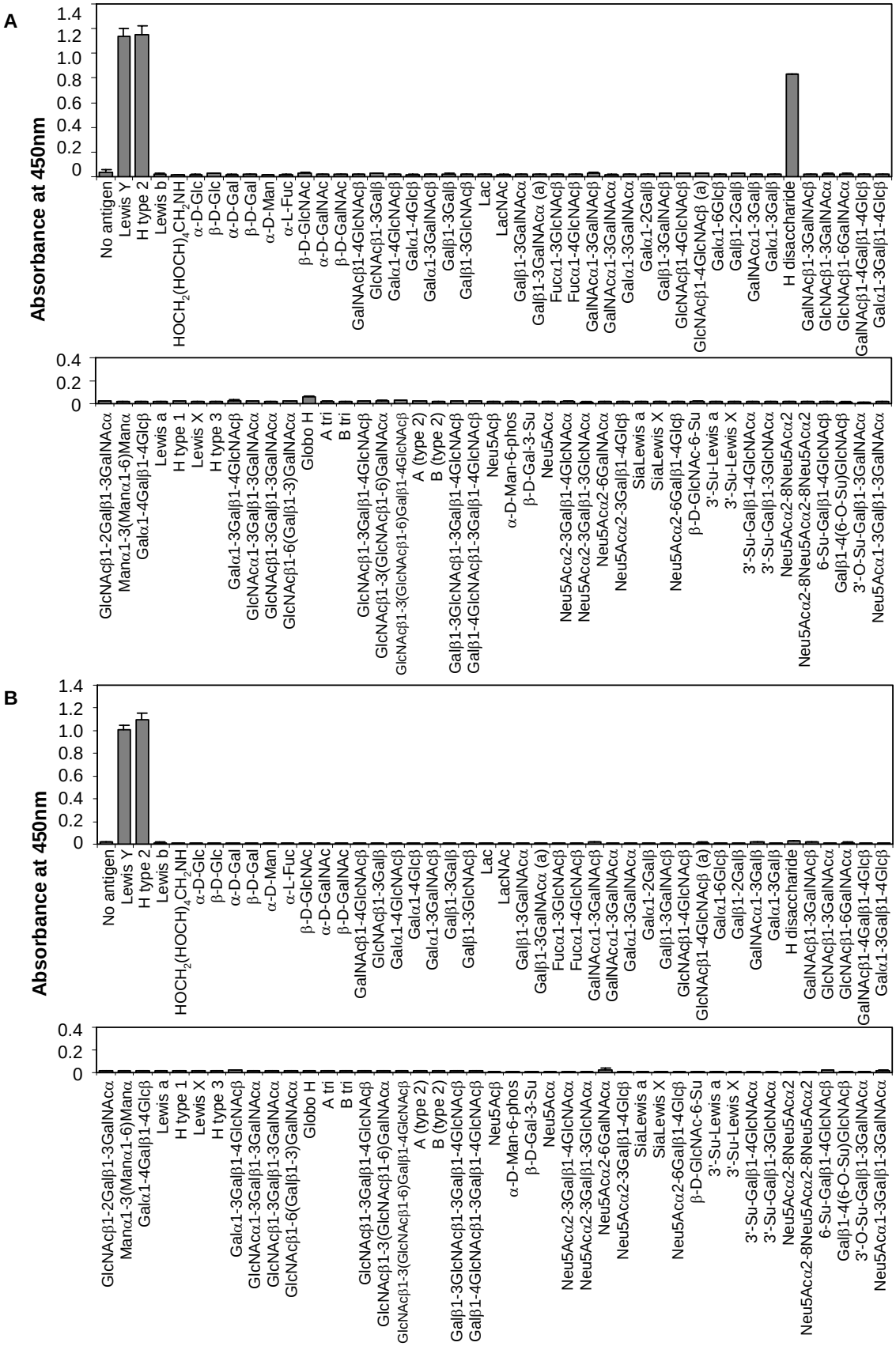

Figure 7: Specificity ELISA with (A) supernatants from the murine hybridoma A51-B/A6 and (B) supernatants from the murine hybridoma A46-B/B10 on 86 different immobilised carbohydrate structures. Supernatants were used undiluted and the signals shown are means of two measurements.

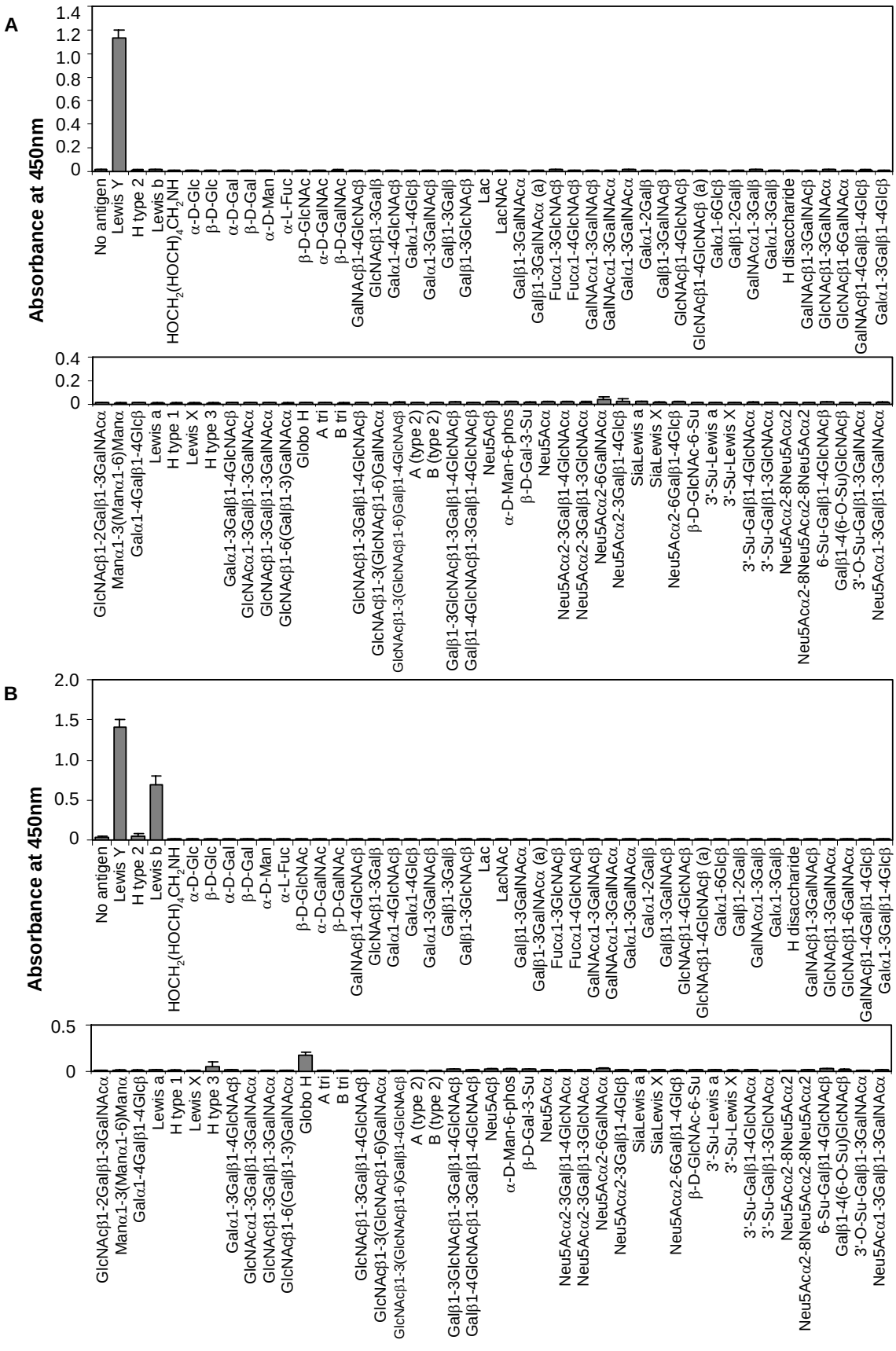

Figure 8: Specificity ELISA with (A) supernatants from the murine hybridoma A70-C/C8 and (B) supernatants from the murine hybridoma A70-A/A9 on 86 different immobilised carbohydrate structures. Supernatants were used undiluted and the signals shown are means of two measurements.

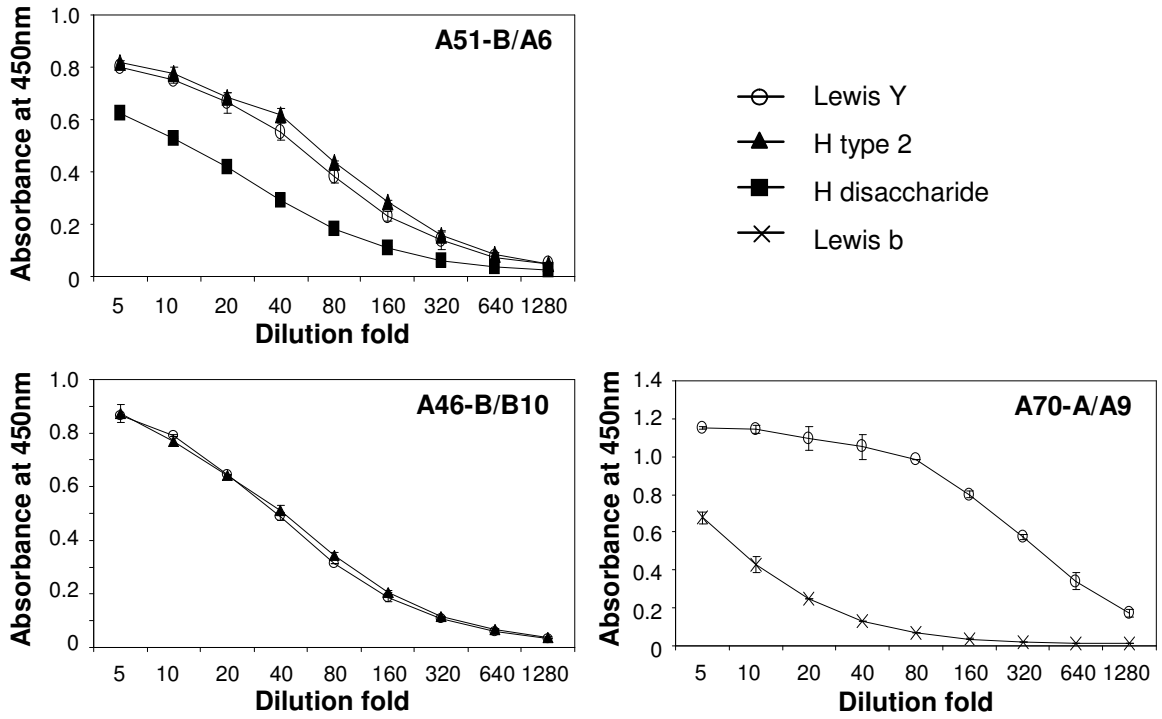

Figure 9: Diagrams showing the concentration dependent binding of A51-B/A6, A46-B/B10, and A70-C/C8 to their respective antigens in ELISA. The dilution fold of the supernatant is given on the abscissa and the ordinate shows A450/630 nm.

2.2 Cloning and sequences of the antibodies

For characterising the VH and VL from the different antibodies the sequences must be obtained and the VH and VL must be cloned in a multistep process. Messenger ribonucleic acid (mRNA) was extracted from the hybridoma clones A51-B/A6, A46-B/B10, A70-C/C8, and A70-A/A9 by use of oligo-dT beads. Complementary deoxyribonucleic acid (cDNA) was produced from the mRNA and polymerase chain reaction (PCR) was subsequently made with cloning primers specific for mouse VH and VL chains. The obtained sequences were aligned with Clustal W (Thompson, Higgins et al. 1994) and the V germline origin was found by IgBLAST search (Altschul, Madden et al. 1997). The sequences are compared without the mutations occurring in the primer region.

In total nine products were successfully cloned. Each VH and VL cloning gave rise to only one product except the PCR product originating from A51-B/A6, which gave rise to two different heavy chains, BA6(1) and BA6(3). Figure 10 shows an alignment of the VH and VL sequences, respectively. The CDRs are defined after Chotia and Lesk, who included only those residues which are not a part of the conserved framework (Chothia and Lesk 1987). The alignment shows that the heavy chains CC8, BA6(1), BA6(3), and AA9 have a high sequence similarity. CC8 and BA6(1) differ by only one amino acid in the framework 3. BA6(3) and AA9 are also very similar in sequence, with eight differences spread from CDR2-CDR3. For the light chains it can be seen that the CC8 sequence differs markedly from the others mostly in the region from framework 1 to CDR2, and that the VL sequences obtained from A51-B/A6 and A46-B/B10 are identical.

Figure 10: Alignment of the heavy- (VH) and light-chain sequences (VL) obtained in the cloning of the antibodies. Red residues are similar in 3-5 sequences; blue residues are similar in 2 sequences; and black residues are unique for the sequence. The sequences are aliged by use of Clustal W. The CDR sequences are blackend fue to patenting reasons.

VH

	Framework 1	CDR1	Framework 2	CDR2	Framework 3	CDR3	Framework 4
CC8	EVKLVESGPELVKPGASVKISCKAS	[redacted]	NIDWVKQSHGKSLEWIGYIY	[redacted]	GTGYNQKFTNKATLTVDKSSSTAYMELHSLTSEYSAVYY	[redacted]	QGTLVTVSA
BA6(1)	EVKLVESGPELVKPGASVKISCKAS	[redacted]	NIDWVKQSHGKSLEWIGYIY	[redacted]	GTGYNQKFTNKATLTVDKSSSTAYMELHSLTSEDSAVYY	[redacted]	QGTLVTVSA
BA6(3)	DVKLVESGPDLVKPGASVKISCKAS	[redacted]	NMDWVKQTHAKSLEWIGYIY	[redacted]	YSDYNQKFTNKATLTVDKSSSTAYMELHSLTSEDSAVYY	[redacted]	QGTLVTVSA
AA9	KVKLQQSGPDLVKPGASVKISCKAS	[redacted]	NMDWVKQTHAKSLEWIGYIY	[redacted]	YSDYNQKFKSKATLTVDKSSSTAYMELHSLTSEDSAIYY	[redacted]	QGTLVTVSA
BB10	QVQLKESGPELKKPGETVKISCKAS	GYTFTNY	GMNWVKQAPGKGLKWMGWIN	TYTG	EPTYADDFKGRFAFSLETSASTAYLQINNLKNEDMATYF	CANDYDGAWFAYWG	QGTLVTVSS

VL

	Framework 1	CDR1	Framework 2	CDR2	Framework 3	CDR3	Framework 4
BB10	DIVMTQTPLTLSVTIGQPASISCKS	SQSLLDSDGKTY	LNWLLQRPGQSPKRLIY	LVS	KLDSGVPDRFTGSGSGTDFTLKISRVEAEDLGVYYCWQ	GTHFPQ	TFGGGTKLEIKRA
BA6	DIVMTQTPLTLSVTIGQPASISCKS	SQSLLDSDGKTY	LNWLLQRPGQSPKRLIY	LVS	KLDSGVPDRFTGSGSGTDFTLKISRVEAEDLGVYYCWQ	GTHFPQ	TFGGGTKLEIKRA
AA9	DIVMTQTPLTLSVTIGQPTSISCKS	[redacted]	LNWLLQRPGQSPKLLIY	[redacted]	NLESGVPDRFSGSGSGTDFTLKISRVEAEDLGVYYCLQ	[redacted]	TFGAGAKLELKRA
CC8	DIVLTQSPLFLHVSLGDQASISCTS	[redacted]	LDWHLQKSDQSLQLLIY	[redacted]	KRNSGVPDRFSGSGSGKDFTLKISRVEPEDLGIYYCFQ	[redacted]	TFGAGTKLEIKRA

Table 2: Germline origins of the V segments for (A) the heavy- and (B) the light chains and the number of residues deviating from the germline sequence in the framework and the CDRs, respectively. Differences, which might be caused by use of a different primer in the N-terminal end, are not included.

A. Heavy chain

Sequence	Germline sequence	Deviation: Framework	Deviation: CDR
BB10	VGK1B	0	0
BA6(1)	VH108A	2	5
CC8	VH108A	3	5
AA9	VH108A	6	4
BA6(3)	VGK1B	5	6

B. Light chain

Sequence	Germline sequence	Deviation: Framework	Deviation: CDR
BB10	bd2	0	0
BA6	bd2	0	0
AA9	bj2	3	6
CC8	cr1	11	9

By making an IgBLAST search it was found that the three VH sequences BA6(1), CC8, and AA9 origin from the same germline V sequence (VH108A) (Table 2), and all show a varying number of deviations from the germline at different positions. The VH obtained from B/B10 turned out to be the original germline sequence VGK1B (Figure 10 and Table 2). Similar to the BB10 VH, the sequence for the BB10 (and BA6) VL proved to be identical to a germline V sequence, namely the bd2 sequence. The sequence of the total A46-B/B10 antibody V segments consequently originates from germline sequences. The two VL sequences AA9 and CC8 are the most mutated of VL sequences and they originate from two different germline V sequences, bj2 and cr1, respectively. The CC8 VL turned out to be mutated at 20 positions when compared to the germline sequence, being by far the V sequence with most variation from the germline (Table 2).

2.3 Expression of antibodies and antibody fragments

In order to verify that the obtained sequences correspond to the antibodies with the observed binding specificities, the VH sequences were subcloned into a human μ chain expression vector. A μ chain vector was chosen for these experiments to obtain multivalent display of the binding sites. The VL sequences were subcloned into a human κ expression vector. Two vectors, a μ and a κ, corresponding to one chimeric IgM (cIgM) antibody, were then transfected into COS-7 cells for transient expression of the antibody. The supernatants were 2-3 days later tested in sandwich ELISA on immobilised anti-human κ antibody and detected with anti-human IgM antibody POD conjugated to verify expression of antibody.

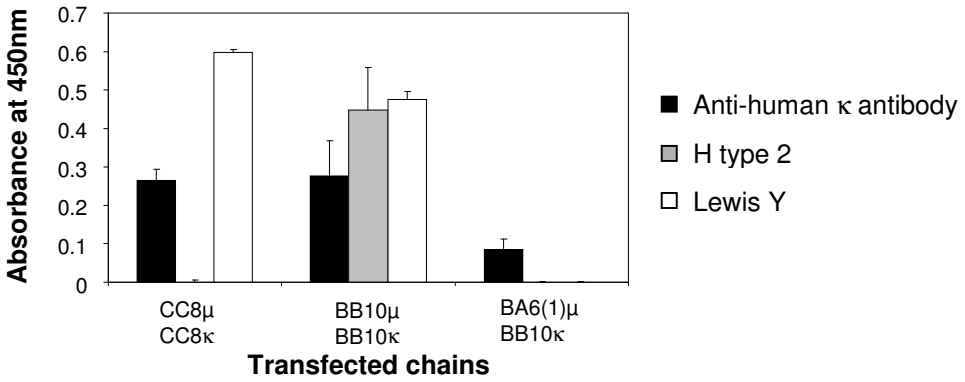

Figure 11: ELISA showing the binding specificity to a few carbohydrates and production of cIgMs from cells transfected with a μ and a κ chain.

Binding experiments were also carried out assaying the produced antibody against Lewis Y and the related carbohydrate structures H type 2, H disaccharide and Lewis b. A representative result of the ELISAs is shown in Figure 11. The cIgM CC8 was produced and bound to the Lewis Y, and not to H type 2 or to Lewis b (not shown). This observed binding correlates nicely with the binding pattern found for A70-C/C8, and indicates that the obtained sequence encodes an antibody with the same specificity as A70-C/C8. The cIgM BB10 clone recognised the H type 2 and Lewis Y. The specificity of cIgM BB10 is on this panel of carbohydrates the same as the A46-B/B10 specificity. In contrast to these antibodies the cells transfected with BA6(1)μ and BB10κ

produced an antibody, but the cIgM was not found to bind to any of the carbohydrates coated in the ELISAs (Figure 11). Successful expression of the cIgM BA6(3) and cIgM AA9 has not been achieved.

The CC8 VH was also successfully cloned into a γ chain expression vector, and as for the cIgMs transient expression of the cIgG was performed by transfecting the γ and κ chains into COS-7 cells. Detection of production and specificity of the cIgG CC8 was made in a similar assay as for the cIgMs with use of anti-human γ POD antibody. Identical results were obtained for production and specificity with the cIgG as for the cIgM. Subsequently, the CC8 μ- and κ- and the γ- and κ- chains, were transfected into CHO cells in order to obtain two stable cell lines, which expressed cIgM- and cIgG CC8, respectively. After successful transfections and clonings larger amounts of cIgM- and cIgG CC8 were obtained. Both the cIgM and the cIgG supernatants were then tested on the panel of 86 carbohydrate conjugates and the specificity of both chimeric antibodies towards Lewis Y was as by the mouse monoclonal antibody A70-C/C8. Figure 12 shows the results.

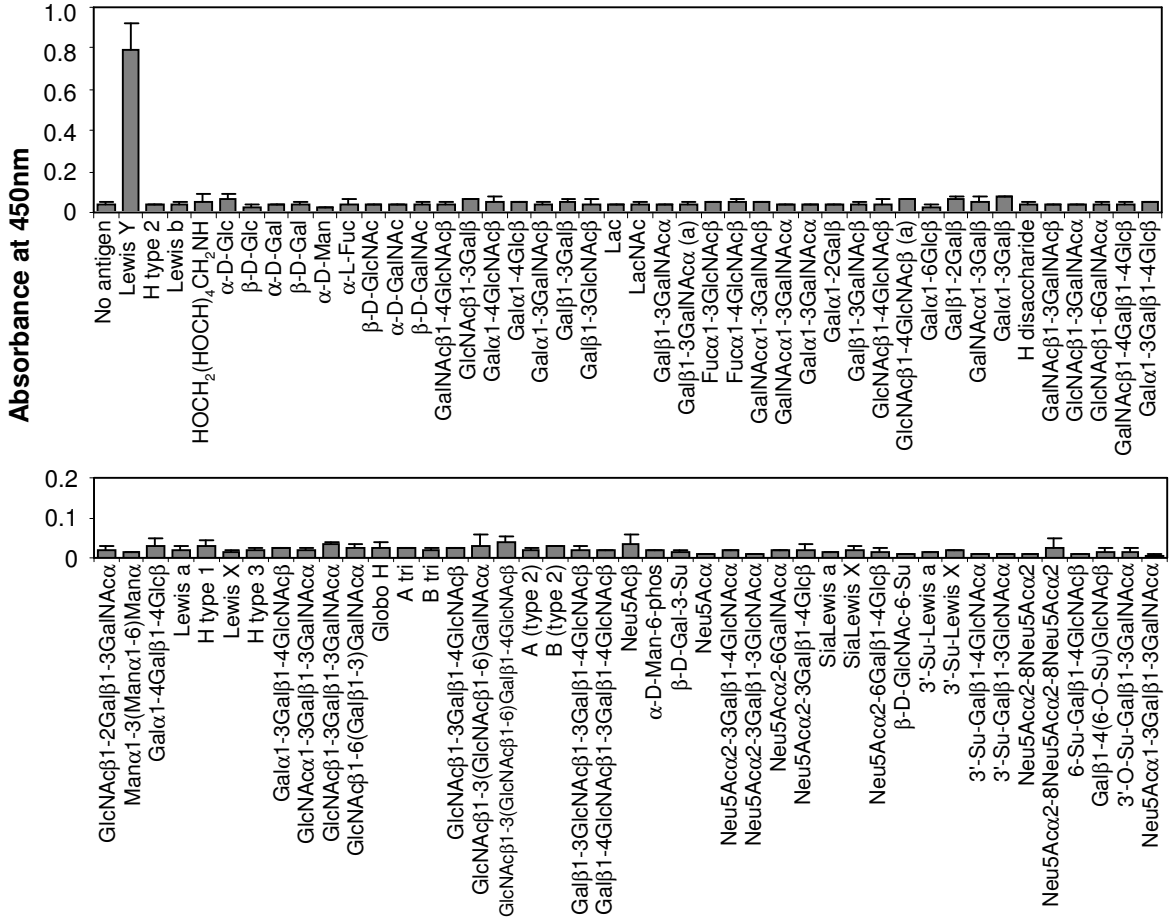

Figure 12: Specificity ELISA with supernatants from stable transfected CHO cells, producing the antibody cIgG CC8, on 86 different immobilised carbohydrate structures. Supernatants were used undiluted and the signals shown are means of two measurements.

The CC8 sequence has furthermore been cloned as scFv with two different linker lengths. The advantages of these formats are that they can be produced in *E. coli* and can easily be purified by use of a His-tag and metal affinity chromatography. The scFv with an 18'mer linker gave a very small response 3 times over background in ELISA when concentrated eluate from the metal affinity chromatography was used and binding was detected with mouse anti-myc-tag and anti-mouse Ig POD antibodies.

The cloning of the scFv with a 1'mer linker was performed as described in (Ravn, Danielczyk et al. 2004). The scFv did express well and showed binding to Lewis Y in ELISA even when tested as crude protein before affinity chromatography. Metal affinity chromatography purified scFv F1-B6 was also tested on the small subset of Lewis Y related carbohydrate structures and detected as the 18'mer linker scFv (Figure 13). Again no cross-reactivity towards the substructures was observed.

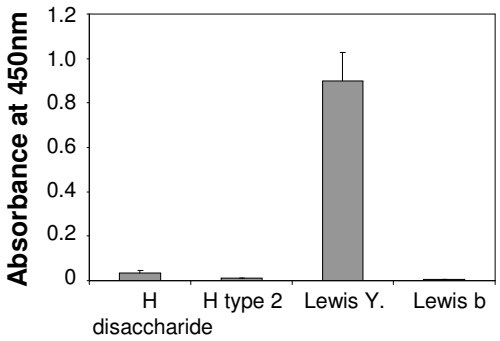

Figure 13: Lewis Y binding of scFvCC8 1'mer linker. Signals are subtracted background.

2.4 Chain shuffling –looking for new specificities

Due to the high similarity of the four antibodies found in both recognition of antigen and sequences, we wanted to generate new antibodies by recombining the obtained VH- and VL- chains. It was also hoped that one of the generated antibodies would bind Lewis Y with higher affinity. This recombination was achieved by transfecting COS-7 cells with all possible combinations of the obtained μ- and κ- chains, for transient expression of the antibodies. The supernatants from the COS-7 cells were tested 2-3 days later in sandwich ELISA on immobilised anti-human κ antibody to verify expression of antibody, and on Lewis Y, H type 2, H disaccharide, and Lewis b for specificity. Binding was detected using an anti-human IgM antibody POD conjugated. The results are summarised in Table 3.

Table 3: Summarising the results obtained from the chain shuffling experiments with respect to expression and specificity of the antibody. + positive result, - negative result, n.d. not done.

Antibody name	VH μ chains	VL κ chains	Expression	Specificity			
				Lewis Y	H type 2	H type disaccharide	Lewis b
AA9/CC8	AA9	CC8	+	+	-	-	-
AA9/BB10	AA9	BB10	+	-	-	-	-
BB10/CC8	BB10	CC8	+	-	-	-	-
BB10/AA9	BB10	AA9	-	n.d.	n.d.	n.d.	n.d.
BA6(1)/CC8	BA6(1)	CC8	+	+	-	-	-
BA6(1)/AA9	BA6(1)	AA9	-	n.d.	n.d.	n.d.	n.d.
BA6(3)/CC8	BA6(3)	CC8	-	n.d.	n.d.	n.d.	n.d.
BA6(3)/AA9	BA6(3)	AA9	-	n.d.	n.d.	n.d.	n.d.
CC8/BB10	CC8	BB10	+	-	-	-	-
CC8/AA9	CC8	AA9	-	n.d.	n.d.	n.d.	n.d.

The result of one of the positive ELISAs is shown in Figure 14. By combining the AA9μ chain with CC8κ chain we obtained an antibody (cIgM AA9/CC8), which when tested on the small panel of carbohydrate conjugates showed the same specificity as the mouse monoclonal antibody A70-C/C8. This suggests that by replacing the light chain in an antibody with broader specificity, with another from an antibody with a similar but narrower specificity, we were able to change the binding pattern within the same group of carbohydrates. In a similar way does the cIgM BA6(1)/CC8 recognise Lewis Y, though generally a weaker signal is seen both for expression and for binding to Lewis Y. The chain shuffled cIgM antibodies CC8/BB10, BB10/CC8, and AA9/BB10 could all be expressed but no binding of the antibody to any of the tested antigens was found. None of the transfection variants containing the AA9 VL or the B/A6(3) VH were found to express an antibody when tested in sandwich ELISA.

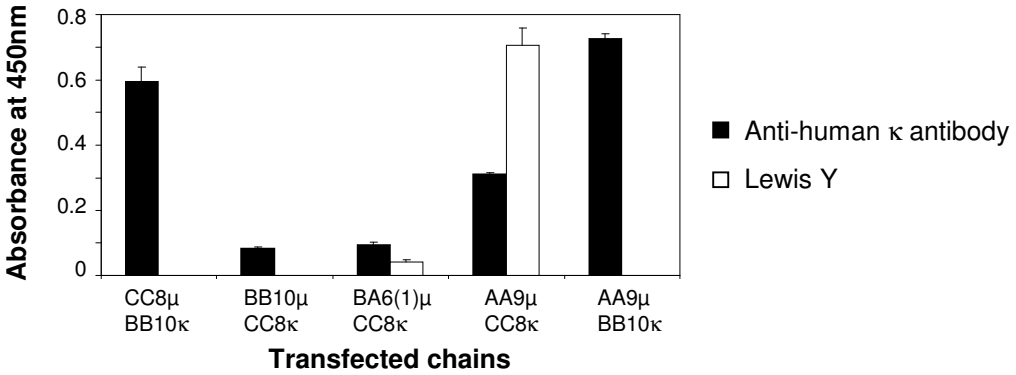

Figure 14: Sandwich and specificity ELISA of supernatants from COS-7 cells transfected with the respective μ and k chains. Legends to the right indicate the immobilised compound. Blank values are subtracted.

The AA9μ chain was combined with the CC8κ chain in CHO cells to obtain a stable cell line expressing the cIgM AA9/CC8 antibody. And subsequently, the AA9 sequence was cloned into a γ expression vector and the AA9γ chain was also combined with the CC8κ chain but for this antibody only transient expression of cIgG AA9/CC8 antibody from COS-7 cells was obtained. Both isotypes were successful expressed, and the supernatants were tested in ELISA on 86 carbohydrate-PAA conjugates and detected with POD coupled anti-human IgG or IgM antibody, respectively. Figure 15 shows the specificity obtained for the cIgG AA9/CC8. Both isotypes bound specifically to Lewis Y and showed no cross-reaction to any of the other immobilised carbohydrates similar to the mouse antibody A70-C/C8.

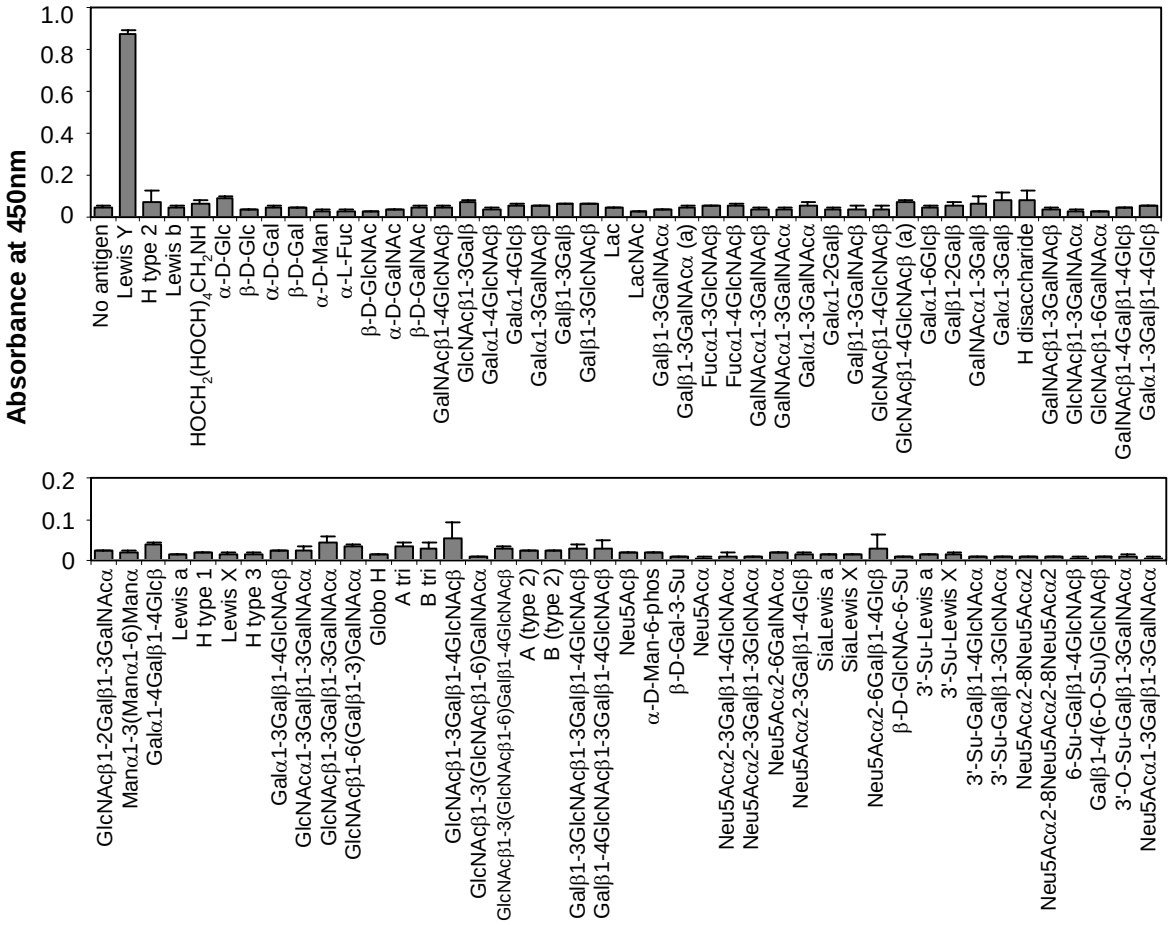

Figure 15: Specificity ELISA with supernatants from transient transfected COS-7 cells, producing the antibody cIgG AA9/CC8, on 86 different immobilised carbohydrate structures. Supernatants were used undiluted and the signals shown are means of two measurements.

2.5 Antibody purification

Four methods were evaluated to purify different antibodies: (1) immunoaffinity chromatography, (2) protein A chromatography, (3) carbohydrate specific affinity chromatography, and (4) ultrafiltration. Pure protein of comparable bioactivity was obtained for the methods 1, 2, and 4. Purifications of the mouse monoclonal antibodies A70-C/C8, A51-B/A6, and A46-B/B10 from the hybridoma supernatants were performed by affinity chromatography on anti-mouse Ig sepharose. Citric acid pH 2.2 into tubes containing 10x PBS pH 7.2 was used for elution. The A70-A/A9 and cIgG CC8 were purified from serum free supernatants on protein A sepharose and eluted by pH 4. After purification the antibodies were subsequently concentrated and rebuffered to PBS by ultrafiltration, leaving pure antibody ready for use. Figure 16 A, B, and C show examples of chromatographic profiles of A46-B/B10 and A70-A/A9 and an SDS-PAGE of the purified proteins, respectively. As seen in Figure 16 C the methods for purifying the proteins result in pure antibodies.

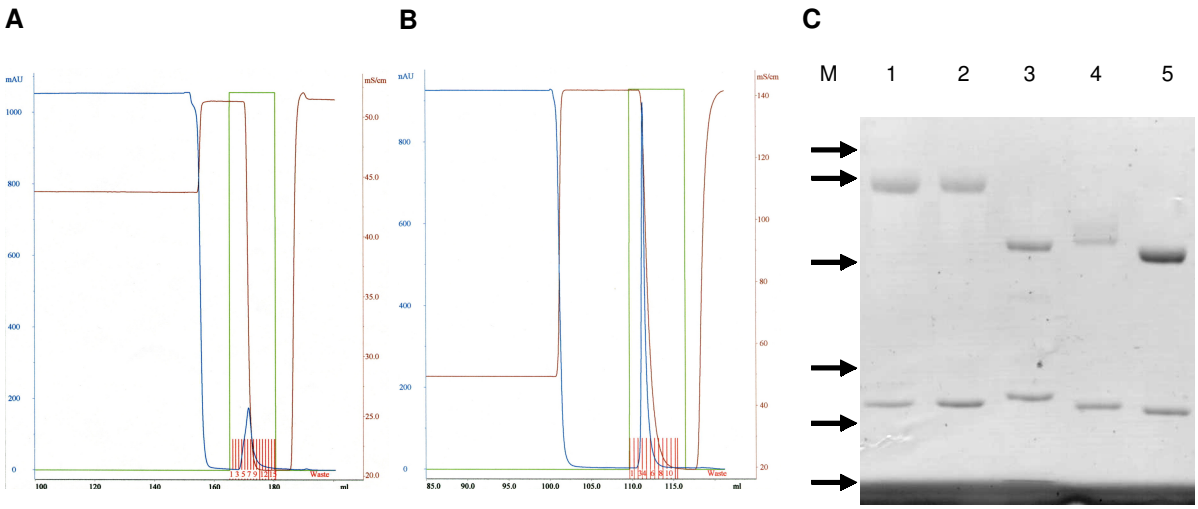

Figure 16: Examples of chromatographic profile from A46-B/B10 on anti-mouse Ig sepharose (A), chromatographic profile from A70-A/A9 on protein A sepharose (B). The blue line is absorbance; the green line is fraction of elution buffer, brown is capacitance, and the red lines indicate collected fractions. (C) Shows an SDS-PAGE of 3µg of the purified proteins. Lane 1 A46-B/B10, lane 2 A70-C/C8, lane 3 cIgG CC8, lane 4 A51-B/A6, and lane 5 A70-A/A9. All protein samples were reduced with β-mercaptoethanol prior to SDS-PAGE analysis. Lane M is prestained marker and arrows indicate the following sizes 113, 93, 50, 35, 29, 21kDa.

The use of a Lewis Y-sepharose affinity matrix was not successful as the different elution conditions tested rendered either the antibody or the matrix inactive. Production of cIgG AA9/CC8 has only been done by transient expression in COS-7 cells, which did not produce enough antibody to establish a purification protocol.

Prolifix is a substitute for serum of plant origin, which contains defined ingredients of low molecular weight. This kind of supplement is of interest in order to produce antibodies without sera and other animal- or human derived material, which poses a potential contamination risk and restricts their use in therapeutic approaches. By use of a defined medium and supplements as Prolifix, chromatographic steps can be replaced by the method ultrafiltration (4). However, these preparations still contain substantial amounts of DNA which has to be removed for most applications, e.g. as it affects the absorbance at 280nm, resulting in a false estimation of

protein concentration. A fast and easy method was therefore developed for DNA removal from preparations of phosphate buffered antibodies purified by ultrafiltration (Christensen, Danielczyk et al. 2004).

This method was originally developed for PankoMab, a murine IgG1 antibody recognising a conformational epitope on MUC1. A common technique to remove DNA contamination is anion-exchange chromatography. However, it was ascertained that interaction of PankoMab with different chromatographic materials like protein A, Sephadex, Sepharose, and Superdex sometimes results in a decrease of the bioactivity of PankoMab of more than 50% (data not shown). Therefore, chromatography is not applicable for PankoMab.

PankoMab was successfully purified from culture supernatants with the serum substitute Prolifix by ultrafiltration followed by rebuffering to PBS. The concentrated and purified antibody preparation was contaminated with substantial amounts of DNA as indicated by the absorption quotient A_{260nm}/A_{280nm} of 1.12. Addition of $MnCl_2$ to 10mM in phosphate buffered antibody preparations and subsequent centrifugation resulted in a DNA-manganese-phosphate co-precipitation and efficient removal of DNA from the solution as indicated by a UV absorption quotient A_{260nm}/A_{280nm} of 0.59 (Table 4).

Table 4: Absorbance values of antibody solution pre precipitation and after addition of $MnCl_2$ to 10mM and centrifugation. Measurements were done on 1:2 dilutions.

	A_{260nm}	A_{280nm}	A_{260nm}/A_{280nm}
Pre precipitation	4.37	3.9	1.12
Post precipitation	0.76	1.28	0.59

Extensive removal of DNA by this procedure could also be shown by electrophoresis on agarose gels (Figure 17 A, lane 2 pre- and lane 3 post-DNA-precipitation), and the DNA was retained in the pellet (Figure 17 A, lane 4). Similar results can be obtained by use of a 1M $CaCl_2$ solution for precipitation, though $MnCl_2$ is preferred to avoid activation of potentially residual existing proteases. The efficiency of DNA removal by addition of $MnCl_2$ is comparable in efficiency to an ion exchange chromatography purified sample with respect to the A_{260nm}/A_{280nm} rate. Purity with respect to other proteins was analyzed by SDS-PAGE (Figure 17 B). Only the heavy and light chain of the antibody could be detected. The SDS-PAGE gel also shows, by comparing the band intensities from lane 1 with lane 2, and lane 3 with lane 4, that apparently no protein was lost during the precipitation. It is assumed that the dramatic change in A_{280nm} is not only caused by DNA removal, but even by co-precipitation of DNA binding proteins, but loading resolved DNA pellet on a SDS-PAGE showed no sign of proteins, which though might be due to low amounts of a specific protein.

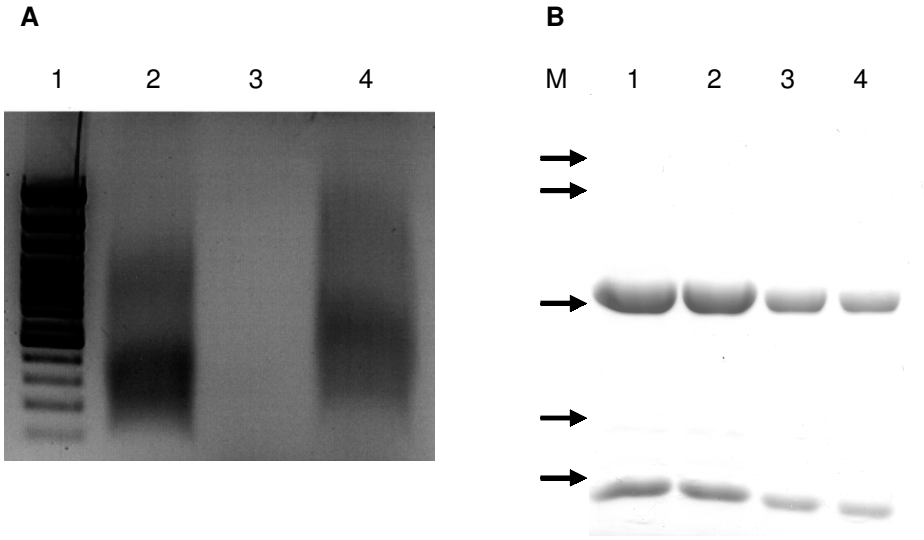

Figure 17: (A) 1.5% agarose gel with EtBr containing: 10µl 100 bp DNA ladder (lane 1), purified PankoMab pre DNA precipitation (lane 2), purified PankoMab post DNA precipitation (lane 3), and pellet from the DNA precipitation resolved in EDTA (lane 4. (B) 10% SDS-PAGE of 10µl PankoMab pre DNA precipitation (lane 1), 10µl PankoMab post DNA precipitation (lane 2), 5µl PankoMab pre DNA precipitation (lane 3), 5µl PankoMab post DNA precipitation (lane 4). All protein samples were reduced with β-mercaptoethanol prior to SDS-PAGE analysis. Lane M is prestained marker and arrows indicate the following sizes 116, 80, 51.8, 34.7, and 30 kDa.

The test for bioactivity and fine specificity of PankoMab using ELISA and detection with anti-mouse Ig POD (Figure 18) proves that the binding activity and the fine-specificity is retained after the precipitation showing a binding to the PDTRP-glycosylated MUC1 peptide with no reduction in activity (Figure 18).

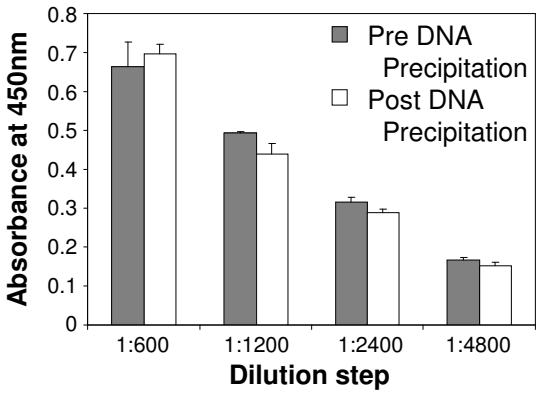

Figure 18: Concentration dependent binding of PankoMab to glycosylated MUC-1 peptide pre- and post-precipitation of DNA.

By ultrafiltration according to this method we were able to successfully purify A70-C/C8 from supernatants of defined media supplemented with Prolifix. The DNA was efficiently removed by adding $MnCl_2$ to a final concentration of 10mM to phosphate buffered antibody preparations. This procedure removes the DNA as a solid precipitate and results in pure A70-C/C8 without affecting its bioactivity, specificity or quantity.

It should be mentioned here that the described method was even successfully applied for removing residual DNA from periplasmic preparations (TES fractions) of bacterially expressed scFv facilitating flow in further chromatographic purification.

2.6 Epitope mapping of the H type 2 carbohydrate

The antibodies A51-B/A6 and A46-B/B10 bind to H type 2 and to some extend to H disaccharide. It was interesting to see whether the differences in the recognition of these two relatively simple carbohydrates could be explored. Experiments were initiated to map the epitopes of the carbohydrates bound by the two antibodies by saturation transfer difference nuclear magnetic resonance (STD NMR) spectroscopy. The STD NMR experiment is based on a transfer of saturation from the antibody to the bound carbohydrate for those carbohydrate protons that interact with antibody protons through an intermolecular nuclear overhauser effect (NOE). By exchange with carbohydrates in solution the saturation of the recent bound carbohydrate can be detected, this means that the dissociation constant for the antibody carbohydrate interaction must be low enough to get a transfer to the carbohydrate and high enough for the carbohydrate to leave the binding site before all magnetisation has been equally distributed between all the protons. All unwanted signals are removed by generating a difference spectrum between an on-resonance spectrum, where the antibody is selectively saturated, and an off-resonance spectrum with an irradiation frequency far from any signal. The protein (large molecule) resonances are removed by recording the spectra with a $T_{1\rho}$ filter consisting of a 30-ms spin-lock pulse prior to acquisition. This leaves transferred saturation signals from the ligand in the remaining spectrum. By using long saturation times and a high excess of ligand (here 5s and 100:1) a preferred difference in amplification is obtained between the most saturated protons and the protons presumably far away from the binding site. The saturation of the individual protons is calculated by dividing with the absolute integrals of a signal in the reference spectra to the absolute integral of the same region in the STD NMR spectra. The saturations are made relative to the most saturated proton. The analyses presented here concerns A51-B/A6 on H disaccharide and H type 2 and A46-B/B10 on H type 2.

The carbohydrates used (H disaccharide and the H type 2) were coupled to a spacer, which acted as a protective group at the reducing end. The spacer were (anomeric C)-O-$CH_2CH_2CH_2NHCOCF_3$. All probes (carbohydrates and carbohydrates with antibody) were prepared by lyophilising them from PBS and resolving them in D_2O 99.9%. A second lyophilisation was made and the probes were resolved in D_2O 99.99% for acquisition of spectra.

Prior to acquiring the STD NMR spectra, 1D, correlation spectroscopy (COSY), total correlation spectroscopy (TOCSY), heteronuclear multiple quantum correlation (HMQC), and HMQC-TOCSY spectra were recorded on pure carbohydrate samples to assign the signals to the individual carbohydrate protons. Generally good spectra were obtained with the resonances well dispersed. An exception to this was the region 3.7-3.85, in which several carbohydrate signals fall. Several signals in this region are not dispersed well enough to assign the individual protons. The amount of resonances that are not dispersed is increasing with increasing number of sugar rings.

2.6.1 STD-NMR on H disaccharide

First A51-B/A6 was analysed against the simplest carbohydrate (H disaccharide) in the STD NMR experiment. Only signals from seven protons could not individually resolved. Figure 19 shows at the bottom the STD spectrum on top of this is the reference spectrum and the assignment of the signals and on the top is the relative absolute integrals shown for the assigned protons. The relative absolute integrals are the ratios of the signals in the STD spectrum to same regions integrated in the reference spectrum, and then normalised to the most saturated integral.

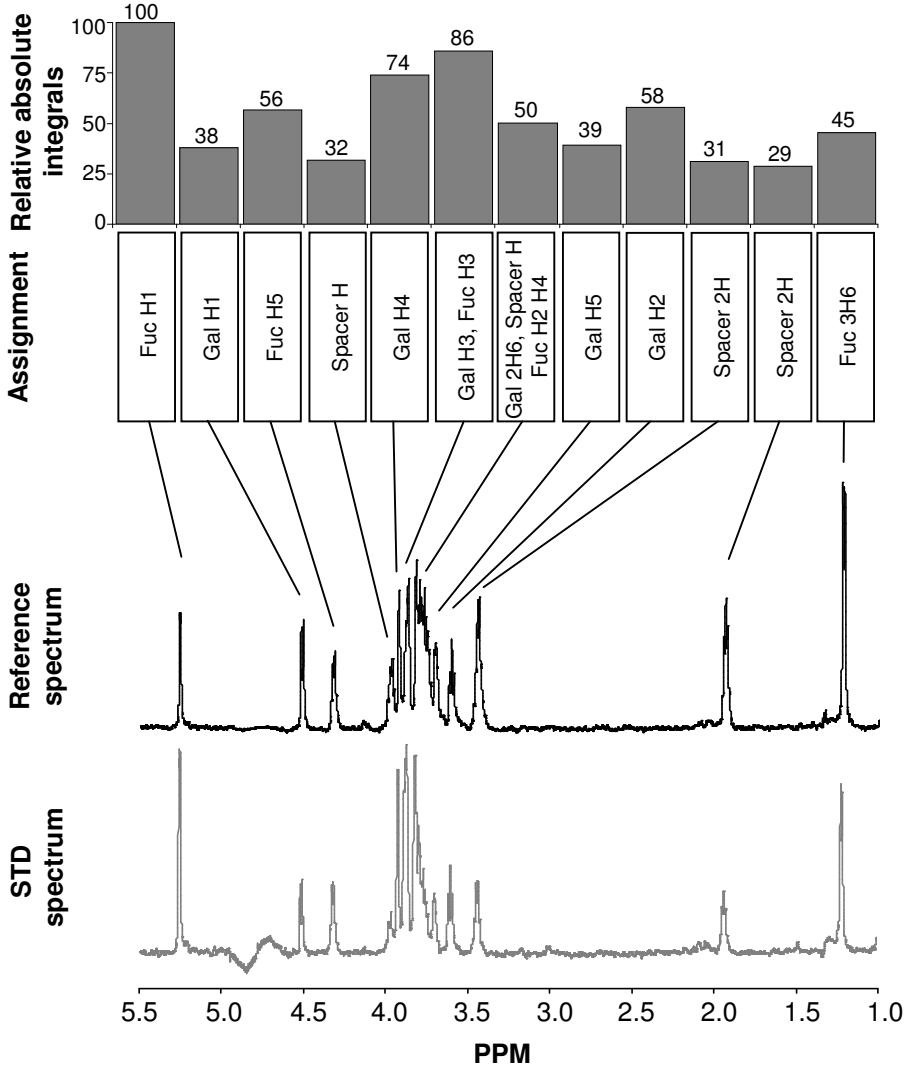

Figure 19: Showing a reference NMR spectrum of H disaccharide with A51-B/A6 in a 100:1 ligand to binding site ratio, at the bottom is the corresponding STD NMR spectrum, and above are the assignment and a diagram showing the relative absolute integrals of the assigned signals.

The spacer protons, which are supposed to be the protons farthest away from the antibody and not be involved in the binding, are saturated to around 30%. The most saturated (100%) and well differentiated proton was found to be the anomeric Fuc H1. Gal H4 is saturated to 74% and thereby also in close contact with the antibody. The differences in saturation found here proved that a clear distinction between the protons with strong

and weak contacts can be made. Gal H3 and Fuc H3 are overlayed and therefore integrated as one and not differentiable and the individual contribution of these protons to the saturation cannot be distinguished. They can either both be strongly saturated (86%) or one stronger and the other weaker. The five signals (spacer H, Fuc H2 H4, and Gal 2H6) are also integrated as one, and as the case is with the Gal H3, Fuc H3 the individual contributions cannot be calculated. The spacer though is only involved to 30% which makes one or more of the remaining signals more saturated than 50%. The remaining protons show intermediate to no influence on the binding. These signals are saturated to between 38 and 58%, and all of them are well separated.

2.6.2 STD-NMR on H type 2

Similar experiments were made with the trisaccharide H type 2 and the antibodies A51-B/A6 and A46-B/B10. Figure 20 shows the STD spectra at the bottom and above them the reference spectra and the assignment. On the top are the relative absolute integrals shown for each experiment with A51-B/A6 (A) and A46-B/B10 (B), respectively. Assigning the resonances for the trisaccharide was more difficult than the disaccharide since more signals occur and 13 signals are not well dispersed. A few extra signals with low intensity showed up in the spectra of the trisaccharide. Especially the peak at 3.1PPM is seen, but a peak is also seen at 2.0PPM. These two protons couple to each other, but not to any of the assigned protons in the spectrum. Since the signals are also present in the STD NMR spectra, the protons must somehow be connected to the sugar moiety. It could be speculated if they originate from an intermediate product in the coupling of the spacer, and therefore be an impurity in the sample provided by the manufacturer.

For the STD NMR experiment with A51-B/A6 a low signal to noise ratio was obtained, which influences the absolute integrals obtained, and thereby the saturation percentages corresponding to the epitope mapping. Figure 20 A shows the spectra and relative absolute integrals with the assignments obtained from the STD NMR experiment with A51-B/A6. The influence of the low signal to noise ratio is already seen in the saturation percentages obtained from three of the spacer H's. The integrals of these three signals from the STD NMR spectra turned out negative, and must origin from the noise level. The remaining three protons (two signals) are saturated with 17 and 28%, respectively. Several signals (GlcNAc H1 H5 H6, Fuc H5, and Gal H1) show a very low saturation with a maximum of 31%. These signals are well dispersed and are therefore not involved in the binding. High saturation of single integrated signals are seen for the protons (GlcNAc 3H8, Fuc H1 and 3H6) with saturation percentages of 74, 63, and 51, respectively. The most saturated signal was found to origin from the Gal H2 GlcNAc H3 peak and the second most saturated signal came from Gal H3 H4 with 93%. Each of these two most saturated peaks was found to contain signals from more than one proton, which makes it difficult to evaluate. The results obtained with the disaccharide showed though that Gal H2 was only intermediately saturated (58%), which leaves the GlcNAc H3 as the major contributor to the STD NMR signal in the trisaccharide spectrum. Similar binding is seen in the disaccharide spectrum, where the Gal H3 is integrated together with Fuc H3, that Gal H4 is saturated to 74%. The saturation percentage increases to 93%, when the Gal H4 is integrated together with the Gal H3. This then indicates that a big contribution to the saturation origin from the Gal H3. Furthermore, it must be taken into account that the relative absolute integrals from the

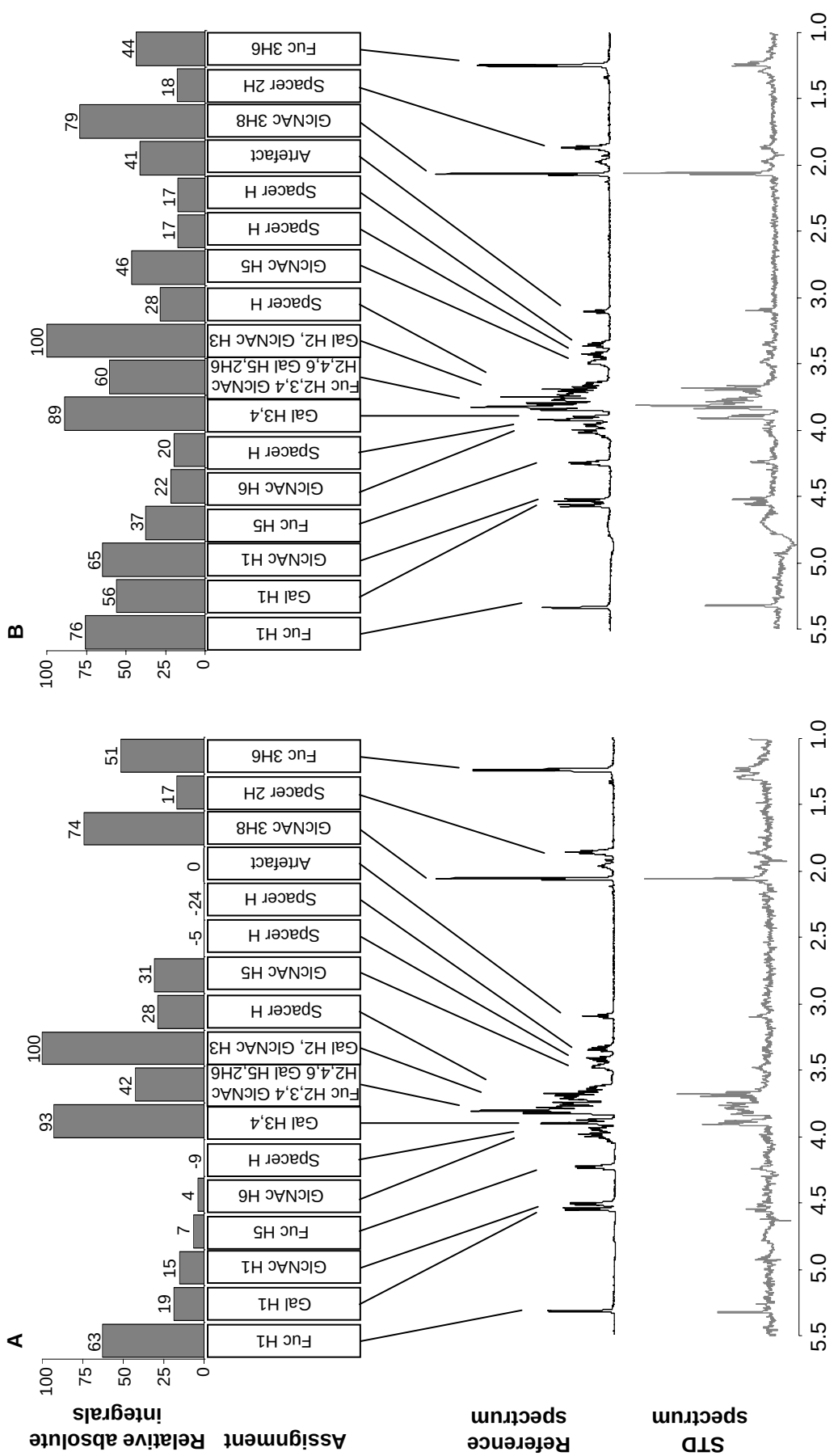

Figure 20: Showing reference NMR spectra of (A) H type 2 with A51-B/A6 and (B) H type 2 with A46-B/B10 both in a 100:1 ligand to binding site ratio, below are the corresponding STD NMR spectra, and above are the assignment and a diagram showing the relative absolute integrals of the assigned signals. In (A) where three of the integrals are negative the curve is cut of at 0 and only the number above the individual signals indicates the value obtained.

disaccharide spectra are relative to Fuc H1, which only show a saturation of 63% in the trisaccharide spectra. Finally, the remaining nine protons are not differentiated but located in the same integral, which is saturated to 42%. As with the previous overlayed signals the individual contributions cannot be evaluated but the results indicate that only minor contributions come from Fuc H3 and Gal H5. This leaves seven protons to share the major contribution to the saturation. This indicates that the increase in affinity observed for A51-B/A6 when the disaccharide is substituted with H type 2 comes from the GlcNAc H3 and the N-acetyl group, whereas an extra fucose on the (GlcNAc C3)-O- is not obstructing the binding or lowering the affinity.

The spectra recorded with the trisaccharide and A46-B/B10 are shown in Figure 20 B along with the assignment and the relative absolute integrals. The STD NMR spectrum did in this case show a better signal to noise ratio than the experiments with the A51-B/A6 antibody and the saturation percentages are in a more trustworthy range as in the disaccharide experiment with A51-B/A6. Here again are the spacer H's saturation below 30% along with one of the GlcNAc H6 protons. Intermediate and low saturation was observed for Gal H1, GlcNAc H1 H5, Fuc H5 3H6, and the artefact already mentioned, all signals are well dispersed corresponding to one integral to one proton. High saturation is seen for the Fuc H1 (76%), Gal H3 H4 (89%), Gal H2 GlcNAc H3 (100%), and GlcNAc 3H8 (79%) protons. The individual proton contributions in the two integrals containing more protons bound to different C atoms cannot be evaluated. This is also the case for the nine protons, saturated to 60%, falling in one integral.

The results from the STD NMR identified similarities and differences in the H type 2 epitopes recognised by the two antibodies A51-B/A6 and A46-B/B10.

2.7 Flow cytometry

Flow cytometric analysis was used to investigate if the antibodies could bind to Lewis Y on the surface of cancer cells and for competition experiments. Several different human cell lines were incubated with a primary antibody and stained with fluorescence labelled secondary antibodies, and the binding of the antibodies to the cell surface was then investigated by flow cytometry. The antibodies included were A51-B/A6, A46-B/B10, A70-C/C8, A70-A/A9, cIgG CC8, cIgG AA9/CC8, and the Globo H specific antibody A69-A/E8 (unpublished additional mouse monoclonal IgM antibody) with secondary antibodies anti-mouse Ig-Cy2 for IgA, anti-mouse IgM-Cy3, anti-mouse IgG-Cy3, and anti-human IgG Fab-Cy3. Furthermore, the lectin UEA I-biotin was included, and detected with streptavidin-Cy3. UEA I recognises almost exclusively terminal fucoses. Control experiments were in most cases made with non-relevant isotype-identical antibodies and secondary antibodies, and in a few experiments unstained cells with secondary antibody only. The data are processed as the X-mean value, which is the mean colour intensity of the total number of cells measured. Figure 21 shows a typical profile for staining of cells. The MCF-7 cells stained in Figure 21 shows X-mean values of 2.6 and 0.4 for colouring with cIgG AA9/CC8 and secondary antibody control, respectively. This gives a mean intensity subtracted background of 2.2. The measured means of intensity are summarised in Table 5.

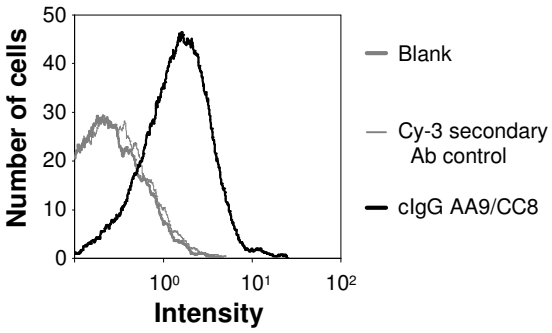

Figure 21: Overlay plot of flow cytometric analysis of MCF-7 cells with cIgG AA9/CC8 and relevant controls.

Four cell lines positive for both A70-C/C8 and A70-A/A9 binding were tested in reversal competition experiments to reveal a concentration dependent inhibition of A70-C/C8 with A70-A/A9 and vice versa. If reversal competition is possible, the two antibodies compete for binding to the same carbohydrate (Lewis Y). The results of the binding and competition experiments are presented in Table 5.

Table 5: Flow cytometric investigation of different cell types and antibody clones. Background was subtracted, and scores grouped according to X-mean values. The groups are defined as (<0 /, 0-0.9 -,1-2.9 +, 3-9.9 ++, 10-15 +++, and >15++++). Abbrevieations: Yes indicates reversal competition and no is no competition, n.d. not determined, m indicate mouse monoclonal antibody, c chimeric mouse/human antibody, UEA I Ulex europaeus lectin -biotin labeled. The values represent at least 2 experiments, except [a] which is only one experiment.

Lectin & antibody		UEA I	mIgA A51-B/A6	mIgM A46-B/B10	mIgM A70-C/C8	cIgG CC8	cIgG AA9/CC8	mIgG A70-A/A9	mIgM A69-A/E8	Reversal competition between A70-C/C8 and A70-A/A9
Specificity		Terminal fucose	H type 2		Lewis Y			Lewis Y, Lewis b, Globo H	Globo H	
Cell line	Type									
K562	L	-	/	-	-	-	-	-	-	-
NM-F9	L	++	/	-	-	-	-	+	-	-
NM-D4	L	+	/	-	-	-	-	-	-	-
LS174T	C	++++	++++	++	++	n.d.	n.d.	++++	n.d.	No
SW480	C	++++	++++	+++	+++	n.d.	n.d.	++++	n.d.	Yes
ZR-75-1	B	++++	++++	+	++	++	+	+++	-	n.d.
T47D	B	++++	++++	++++	+++	++	++	++++	-	Yes
MCF-7	B	++++	++++	++	++	+[a]	+	++++	++	No
HEK293	K	++++	++++	+	-	n.d.	n.d.	-	n.d.	-

B Breast carcinoma
C Colorectal carcinoma
L Myelogenous leukemia cell line
K Kidney cells transformed with adenovirus 5 DNA

The colon and breast carcinoma cell lines proved to be positive in binding of all Lewis Y binding antibodies. The MCF-7 cell line shows expression of both Lewis Y and Globo H, whereas no conclusions can be drawn on Lewis b. The reversal competition between A70-A/A9 and A70-C/C8 for the SW480 and T47D indicates that these cell lines express only Lewis Y on the cell surface. For LS174T no inhibition was seen, which along with the lack of Globo H testing makes further conclusions on antigen expression impossible.

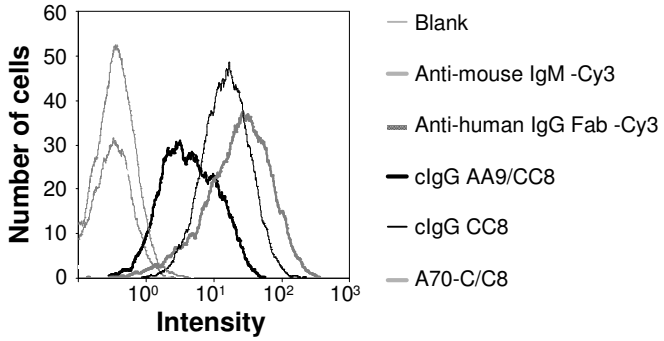

Figure 22: Overlay plot of flow cytometric analysis of T47D cells coloured with no antibody, anti-mouse IgM-Cy3 only, anti-human-IgG Fab-Cy3 only, cIgG CC8, cIgG AA9/CC8, or A70-C/C8 all with their respective secondary antibodies.

A comparison of the cell binding observed for A70-C/C8, cIgG CC8, and cIgG AA9/CC8 as summarised in Table 5 and represented by the overlay plot of staining of T47D cells in Figure 22 shows that all three antibodies obviously recognise the same antigen. Furthermore, it can be seen that the IgM generally stains the Lewis Y expressing cells more intense, which was also expected due to a higher avidity and the possible binding of more than one secondary antibody per IgM compared to an IgG. The binding of cIgG CC8 and cIgG AA9/CC8 to the Lewis Y expressing cells are in the same order of magnitude.

Surprisingly, it was found that the NM-F9 cells revealed binding of A70-A/A9 as shown in the overlay plot (Figure 23), in contrast to NM-D4 and K562 cells which did not bind A70-A/A9. None of these three cell lines reacted with the Lewis Y specific antibody A70-C/C8 or the Globo H antibody (A69-A/E8). This suggests that the sub line NM-F9 displays Lewis b. The presence of terminal fucoses was further underlined by stronger binding of UEA I to the NM-F9 cells than to K562 and NM-D4.

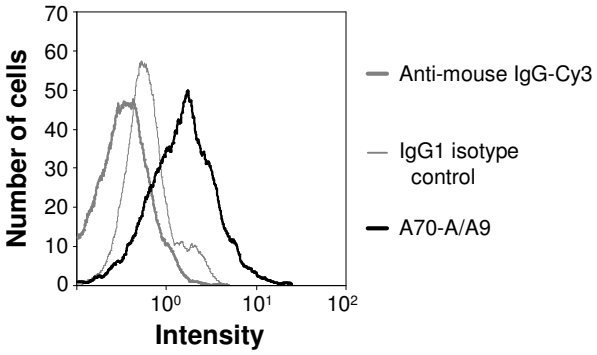

Figure 23: Overlay plot of flow cytometric analysis of NM-F9 cells coloured with anti-mouse IgG-Cy3 only, IgG1 isotype and secondary antibody, or A70-A/A9 and secondary antibody.

Binding of the lectin UEA I and A51-B/A6 to HEK293 show the presence of fucose. Furthermore, a weak interaction with A46-B/B10 was found as well. This indicates the presence of an epitope involving the H type 2 or at least the H disaccharide.

The X-mean values from A51-B/A6 subtracted unspecific IgA binding resulted in negative values. The measuring of H type 2 on the K562 cells and sub cell lines thereof could not be made with A51-B/A6. The use of an IgA antibody on these cells was therefore not possible to identify interesting carbohydrates. Presumably, an Fcα receptor is expressed on the cell surface of these cells.

2.8 Immunocytochemistry

For further investigating the binding of the original and modified Lewis Y binding antibodies 13 cell lines was stained by use of immunocytochemistry. The cells were immobilised on slides and stained by binding of antibodies A70-C/C8, A70-A/A9, cIgG CC8, and cIgG AA9/CC8. Visualisation was done with anti-mouse IgG/IgM-Cy3, or anti-human Ig-FITC. Background staining was determined with secondary antibody only.

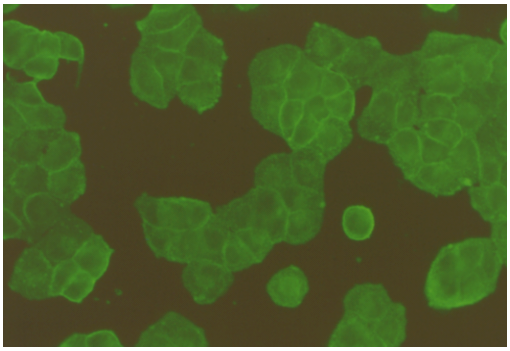

Figure 24: Example of cell staining with A70-A/A9 on T47D cells. Anti-mouse IgG/M-FITC was used as secondary antibody.

The results of the cell stainings are summarised in Table 6. In Figure 24 is as example the staining of T47D cells with A70-A/A9 shown. The Figure shows that the antibody staining gave rise to a strong, surface located, and equal distributed colouring of the T47D cells.

As seen in Table 6, four cell lines (OVCAR-3, HCT15, MCF-7, and MT-3) were positive in binding of all antibodies. In these four cases a less intense colouring was found when the cIgG CC8 was applied compared to the other used antibodies. Two cell lines (T47D and H184A1) were only tested with one or two antibodies but they were both found to be positive in staining. The HCT 116 cells showed only staining with the cIgGs, whereas the mouse IgM and IgG did not bind. This could indicate an artefact even though the background has been subtracted. The mammary ductal carcinoma (MDA-MB 435) and the ovarian ascites adenocarcinoma (SK-OV-3), and the (JEG-3, H-29, HepG2, and U266) were all negative for all four antibodies tested.

Table 6: Immunocytochemistry staining of different cell types. A colouring score over the background is given from no colouring (-) to maximum colouring (+++). Abbreviations: n.d. not done, [B] high background coloring, m mouse monoclonal antibody, c chimeric mouse/human antibody.

Antibody		mIgM A70-C/C8	cIgG CC8	mIgG A70-A/A9	cIgG AA9/CC8
Specificity		Lewis Y	Lewis Y	Lewis Y, Lewis b, Globo H	Lewis Y
Cell line	type				
OVCAR-3	O	++	+ [B]	++	+++ [B]
SK-OV-3	O	-	- [B]	-	- [B]
HepG2	H	-	-	-	-
MDA-MB 435	B	-	- [B]	-	- [B]
HCT 116	C	-	+	-	+
HCT15	C	++	+	++	++
HT29	C	-	- [B]	-	- [B]
MT-3	B	++	+	++	++
MCF-7	B	+++	+	++	++
T47D	B	+++	n.d.	+++	n.d.
U266	Y	-	- [B]	-	- [B]
JEG-3	P	-	-	-	-
H184A1	N	++	n.d.	n.d.	n.d.

B Breast carcinoma
C Colorectal carcinoma
H Hepatocellular carcinoma
O Ovary carcinoma
P Placenta, choriocarcinoma
Y B lymphocyte; plasmacytoma, myeloma
N Non-tumorigenic breast epithelial cell line

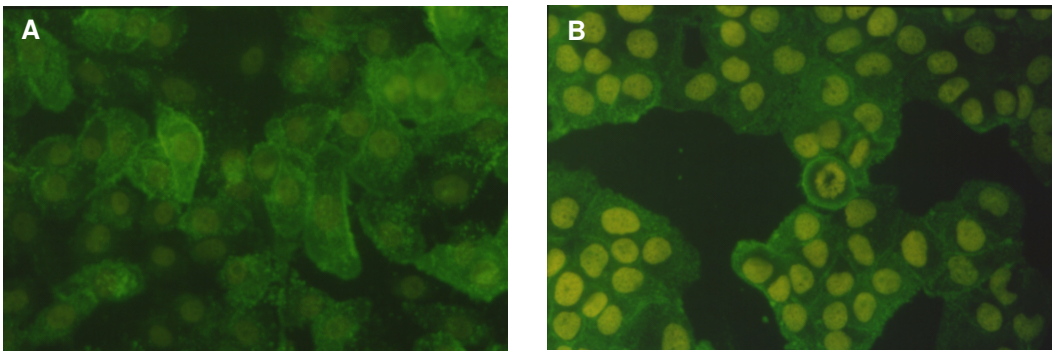

Figure 25: Examples of cell stainings with (A) A70-C/C8 on H184A1 cells (B) A70-C/C8 on T47D cells. Counter staining of the nucleus was made with DAPI and anti-mouse IgG/M-FITC was used as secondary antibody.

The staining of the non-tumourigenic breast epithelial cell line, (H184A1), with A70-C/C8 and 4'-6-Diamidino-2-phenylindole (DAPI) showed a differentiated staining of the cells (Figure 25 A). Not all cells are stained and they are not coloured equally well. In contrast, the breast carcinoma (T47D) cells stained with A70-C/C8 and DAPI shown in figure 25 B showed that all the immobilised cells expresses Lewis Y. Furthermore, all cells are stained with equal intensity.

2.9 Affinity measurements

Surface plasmon resonance (SPR) technology on a BIACORE 2000 with Streptavidin Sensor Chip SA was used to estimate antibody affinities. In the SPR detection system one of the ligands is attached directly to the surface of a sensor chip, here via the biotin-streptavidin interaction. The analyte flows over the surface and is in solution. The SPR response measured is proportional to the mass of the analyte that during binding in real time accumulates at the surface of the chip. Experimental conditions of high density of multivalent carbohydrate-PAA-biotin immobilised on the sensor chip were used to allow multivalent binding of the antibodies to the carbohydrates. The affinities obtained are functional affinities (K_{obs}) (avidity), an expression for the overall affinity of the antibody towards e.g. a cell displaying the antigen multivalent (Karush 1970; Rheinnecker, Hardt et al. 1996).

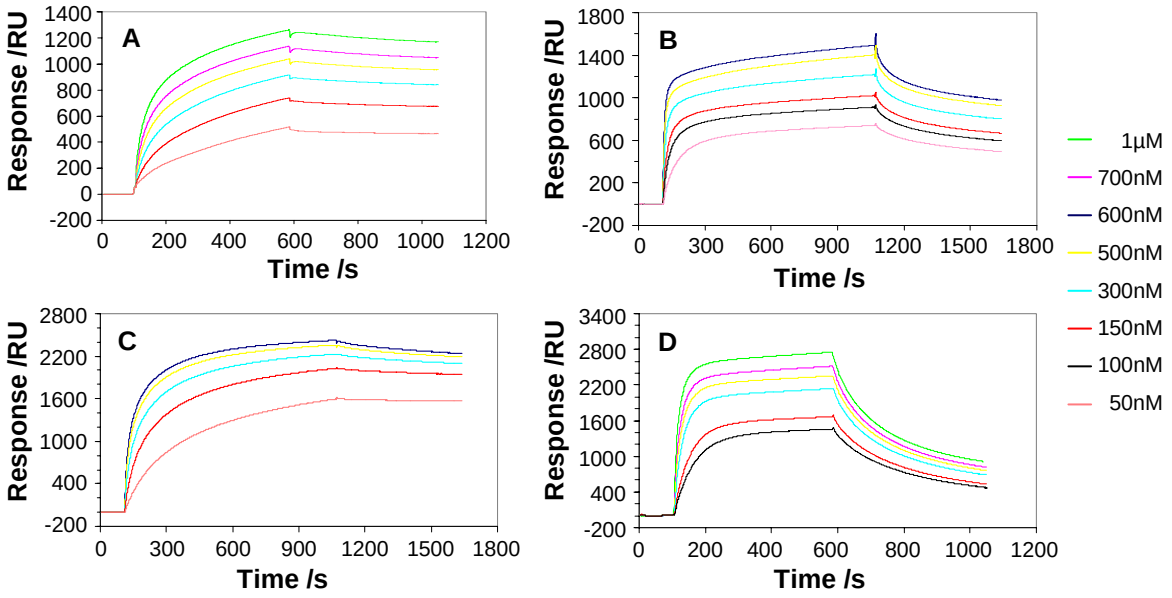

Figure 26: Sensorgrams obtained from the SPR analysis on Lewis Y with (A) A51-B/A6, (B) A46-B/B10, (C) A70-C/C8, and (D) A70-A/A9. B and C has double the analyte injection time as does A and D.

Figure 26 shows examples of measured binding curves for the mouse monoclonal antibodies A51-B/A6 (A), A46-B/B10 (B), A70-C/C8 (C), A70-A/A9 (D) to immobilised Lewis Y. The individual functional affinities for each antibody and the different carbohydrates were calculated according to the Langmuir 1:1 (BIAevaluation software, Biacore, Sweden). K_{obs} values are summarised in Table 7.

Table 7: Binding curves were obtained by SPR analysis, and functional affinities (given as K_{obs} (M)) were calculated on BIAevaluation software using the Langmuir 1:1 model, global fitting. n.r.d. no response detected. The K_{obs}s are means of two sets of data measured on different chips.

Carbohydrate / Antibody	H type disaccharide	H type 2	Lewis Y	Lewis b	Globo H
A51-B/A6	1×10^{-8}	5×10^{-9}	4×10^{-9}	-	-
A46-B/B10	n.r.d.	4×10^{-9}	7×10^{-9}	-	-
A70-C/C8	-	-	2×10^{-9}	-	-
A70-A/A9	-	-	6×10^{-8}	2×10^{-7}	n.r.d.
cIgG CC8	-	-	10^{-6}	-	-

The functional affinities of the IgMs A46-B/B10 and A70-C/C8 and the IgA A51-B/A6 to the Lewis Y structure are of the same order of magnitude, whereas the IgG A70-A/A9 binds with an approximately 10 fold lower affinity (Table 7). A51-B/A6 and A46-B/B10 also bind to H type 2 with similar functional affinities. Binding to the H disaccharide was only detected with A51-B/A6 and the functional affinity to this carbohydrate was found lower than to H type 2, which furthermore supports the hypothesis that there might be a determinant in the GlcNAc contributing to binding. In a similar way A70-A/A9 was found to bind to the Lewis b carbohydrate with lower functional affinity than when tested on Lewis Y. No response was observed when the analyte A70-A/A9 was tested on a chip with immobilised Globo H.

The response levels for the cIgG CC8 were low for all the tested concentrations and each concentration reached a steady state. A calculated K_{obs} value for this antibody is approximately 500 fold lower than for the A70-C/C8. This lower binding is caused by the divalent versus multivalent binding difference in the IgG to IgM.

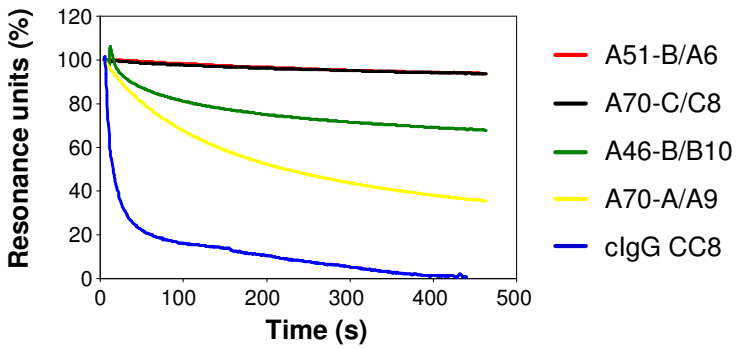

Figure 27: Overlay plot of individual dissociation curves on Lewis Y for A70-C/C8, A51-B/A6, A46-B/B10, A70-A/A9, and cIgG CC8 all with an antibody concentration of 500nM. All curves are relative to the individual signals at the end of the association curve. A51-B/A6 and A70-C/C8 are almost identical.

The functional affinities to Lewis Y are in the range from approximately 0.5nM to approximately 5nM determined for all the murine antibodies, with the IgG having the lowest functional affinity. Comparing the dissociation curves on Lewis Y (Figure 27), striking differences can be seen. The A70-C/C8 and the A51-B/A6 shows virtually no dissociation, whereas intermediate dissociation is seen for A70-A/A9 and A46-B/B10 and almost instant dissociation is seen for cIgG CC8. Due to the 10-12 binding sites of the IgMs compared to four and two for IgA and IgG, respectively, the avidity, rebinding or corporate binding is expected to play a large role for the functional affinities.

Since cIgG AA9/CC8 has not been successfully purified, no SPR measurements could be performed. Therefore, an ELISA comparison was made. The amounts of produced antibody in the supernatants containing cIgG CC8 and cIgG AA9/CC8 were determined by sandwich ELISA on coated anti-human κ antibody. Figure 28 shows the ELISA result on Lewis Y of cIgG CC8 and cIgG AA9/CC8 supernatants diluted to equal antibody concentrations as evaluated in sandwich ELISA.

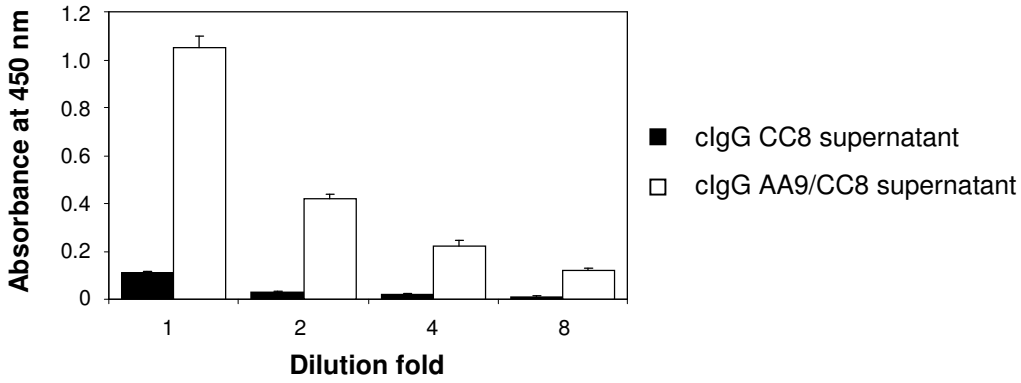

Figure 28: A comparison ELISA of the activities of cIgG CC8 and cIgG AA9/CC8 with equal relative concentrations of the antibodies. Solid phase antigen was Lewis Y-Paa conjugate and bound antibody was detected with anti-human γ antibody POD coupled.

In the Lewis Y ELISA it was found that the signal intensities of cIgG AA9/CC8 were approximately 10 times higher than of cIgG CC8 at a given dilution. This also means that equal signal intesities are obtained when comparing the 1:8 diluted cIgG AA9/CC8 with the 1:1 diluted cIgG CC8 (Figure 28). Signals indicate bound antibody which means that comparable signals of 10 fold different concentrations reflect differences in affinity (Yelton, Rosok et al. 1995).

2.10 Mimicry between histone H1 and a mixed carbohydrate epitope

Looking for Lewis Y expression on different types of tumour cells we found in cases of slides stored at minus 20°C a diffuse staining of the cell nucleus with the antibody A70-A/A9. The staining could be a hint of an antibody cross-reactivity to a nucleus protein because freezing breaks the cell membrane and allows antibody diffusion inside the cell. Therefore a possible binding was investigated to histones, which are a major group of nucleus proteins. Commercially available bovine bovine histone H1 was coated for ELISA experiments and all

four mouse monoclonal antibodies A51-B/A6, A46-B/B10, A70-C/C8, and A70-A/A9 were analysed for their binding behaviour to this protein. Binding was detected with anti-mouse Ig POD coupled antibody.

The initial ELISA showed that A70-A/A9 bound to bovine H1 whereas none of the other antibodies tested were positive. As the nucleus also contains proteins with glycosylations (Wells, Vosseller et al. 2001), it was further investigated if the binding of A70-A/A9 to the bovine histone H1 was carbohydrate dependent. A microtiterplate was immobilised with bovine histone H1 and Lewis Y conjugate, which prior to primary antibody incubation was periodate oxidized according to (Woodward, Young et al. 1985). This oxidation cleaves the ring structure of carbohydrates in-between vicinal hydroxyl groups without altering the structure of the polypeptide chain. The binding of A70-A/A9 to bovine histone H1 proved to be independent of periodate oxidation, whereas the binding to Lewis Y conjugate was sensitive to periodate oxidation (Figure 29). Additionally the binding behaviour of the antibody A46-B/B10 under identically conditions was investigated as a control. No binding to bovine histone H1 was measured at all with or without periodate oxidation, but binding was also sensitive to periodate oxidation against the Lewis Y-PAA conjugate. A subsequent staining of periodate treated T47D cells showed no nuclear staining with A70-A/A9, whereas a control anti-human H1.2 antibody did show a speckled colouring pattern inside the nucleus (data not shown).

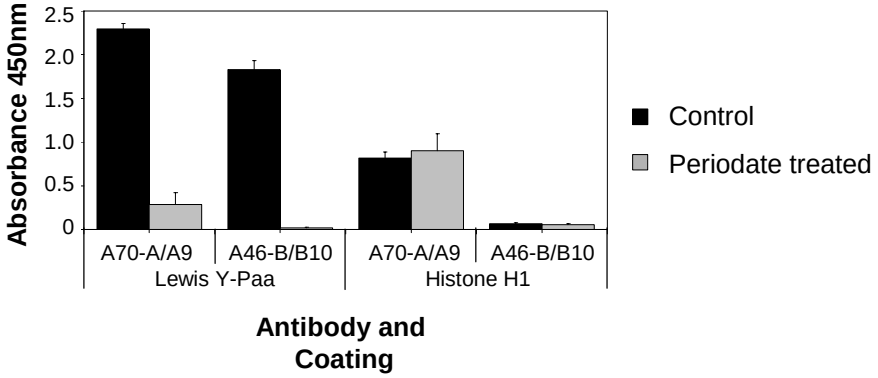

Figure 29: ELISA on periodate- and non- periodate oxidized bovine histone H1 and Lewis conjugate with A70-A/A9 and A46-B/B10. Gray bars indicate periodate treated wells, and black bars indicate control (not periodate treated wells).

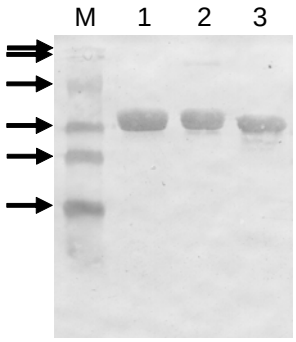

Figure 30: Western blot of a 15% SDS-PAGE loaded with 20µg natural mixture of the histones H1, H2A, H2B, H3 and H4 from calf thymus (lane 1), 4µg of histone H1.2 recombinant human (lane 2), and 4µg of histone H1 from calf thymus (lane 3). Lane M is prestained marker and arrows indicate the following sizes 116, 80, 51.8, 34.7, 30, and 22 kDa. The blot was incubated with A70-A/A9.

Moreover bovine histone H1 recognition by A70-A/A9 was also investigated by Western blot (Figure 30, lane 3). Additionally a natural mixture of the bovine histones (H1, H2A, H2B, H3, and H4) (Figure 30, lane 1) and the human histone H1.2 (Figure 30, lane 2) was included in the blot. Figure 30 shows that only the histone H1's are detectable in the blot, independent of the H1 species.

To estimate the relative binding affinity of A70-A/A9 towards histone H1 in comparison to Lewis b a cell inhibition assay was performed with NM-F9 cells, which express Lewis b (see flow cytometry chapter 2.7). Soluble Lewis b as well as human histone H1.2 were used as competitors of binding of ^{51}Cr labelled NM-F9 cell to wells coated with A70-A/A9. The obtained curves of inhibition are shown in Figure 31 and the IC50 values read from these curves were found to be for human histone H1.2 and Lewis b 0.012mM and 0.17mM, respectively. From these experiments a 15 fold higher affinity of the antibody to H1 than to Lewis b was calculated. In addition, the Lewis Y- and Lewis b-PAA-conjugates inhibited strongly the cell adhesion (about 90% at a concentration of 7µg/ml) whereas the Globo H-PAA-conjugate was without effect at this concentration. The chain shuffling variant cIgG AA9/CC8 has also been tested on bovine histone H1. No signal was detected in ELISA by use of this antibody, which is in accordance with the results of A70-C/C8. Both antibodies recognize highly specific the Lewis Y epitope.

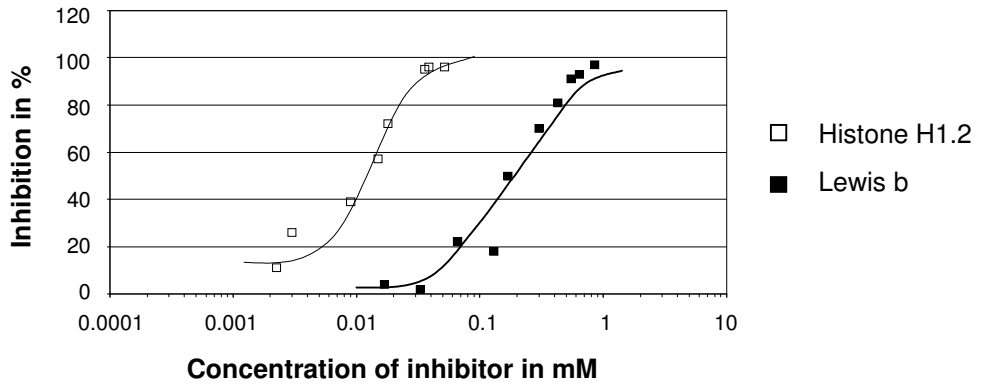

Figure 31: Inhibition experiments of A70-A/A9 binding to NM-F9 cells through addition of human histone H1.2 or Lewis b.

2.11 Anti-idiotypic antibodies

Anti-idiotypic antibodies have generally been generated by immunising mice with the idiotype. We here set out to develop a method which could generate a large amount of different anti-idiotypic antibodies from phage display libraries. Chapter 2.11.1 concerns the development of the method for selection of anti-idiotypic antibodies of large diversities. The method is developed on the Lewis Y specific mouse monoclonal antibody A70-C/C8 (IgM, κ). The method of generation of large diversities was further investigated on antibodies with different specificities compared to A70-C/C8: On A70-B/B10 (IgM, κ) which recognises Lewis Y and H type 2, PankoMab (IgG1,κ) which recognizes an unique carbohydrate induced conformational epitope, the MUC1 antigen, and A78-G/A7 (IgM,κ) which recognizes the pan-carcinomic Thomsen-Friedenreich disaccharide, TF-

antigen (Karsten, Butschak et al. 1995). Chapter 2.11.1 furthermore concerns the inhibition potential of the anti-idiotypic antibodies selected on A78-G/A7 and Pankomab. The chapter 2.11.2 describes the inhibition potential and the nature of the anti-idiotypic antibodies selected on A70-C/C8 and A46-B/B10. A new presentation of the anti-idiotypic antibodies to the immune system is outlined in chapter 2.11.3

2.11.1 Selection method for mimicry antibodies

Phage display selections on A70-C/C8 with the Tom J library were used to isolate anti-idiotypic antibodies. Five different elution methods were compared for the ability to generate anti-idiotypic scFv. Elution with acidic glycine buffer, pH 2.2, was used for non-specific elution as being independent of antibody specificity. Specific elution was performed with high concentrations (100µg/ml) of the Lewis Y polyacrylamide conjugated (Lewis Y-PAA). In addition both procedures were carried out with or without subsequent treatment of the eluted phage with trypsin. The rationale behind the trypsin treatment is cleavage of modified p3 originating from the helperphage KM13, rendering phage without scFv non-infective (Figure 4). Tryptic treatment of the phagemid scFv libraries showed that only about 1% of the phage carry scFv. The fifth method evaluated was direct proteolytic elution via tryptic cleavage of the myc tag of scFv, also rendering phage without scFv non-infective (Figure 4)(Goletz, Christensen et al. 2002).

Table 8 shows the overall results of these experiments. The number of colonies obtained from the first round of selection was highest with the non-specific pH elution. It was considerably reduced by subsequent tryptic cleavage of the eluted phage. Specific elution with the Lewis Y-PAA resulted in less than 3% of the number of phage eluted non-specifically; however, it still elutes a large portion of phage without scFv, as shown by subsequent trypsin treatment. Specific elution combined with subsequent trypsin treatment resulted in less than 0.065% of the number of phage eluted non-specifically. The proteolytic elution alone yielded about twice the amount of phage compared to the lowest achieved number with the combined specific elution and subsequent trypsin treatment. Comparing the various elution methods the number of colonies achieved after the second rounds of selection did not show consistent increase from the first round, which, however, did not reflect the positive enrichment of specific scFv-phage.

By far the highest enrichment of anti-idiotypic scFv-phage over two rounds of selection was achieved with the combined specific elution and subsequent trypsin treatment of eluted phage, yielding 28 anti-idiotypic scFv-phage out of 96 tested clones. Simultaneously, the number of phage binding to other parts of the immunglobulins decreased. This was also the case for the antigen specific elution alone, but the enrichment of the wanted anti-idiotypic scFv was, if at all, only very little resulting in 2 clones out of 96.

To test if the specific elution was able to elute all anti-idiotypic scFv-phage the phage remaining on the antibody coated beads after a specific elution was eluted by a proteolytic elution. Testing of 96 clones from this elution did not reveal a single anti-idiotypic binding and indicates that the specific elution was able to elute all anti-idiotypic scFv-phage.

Table 8: Comparison of the effect of different elution techniques on the yields of specific anti-idiotypic scFv-phage versus other types of bound phage. Selections were performed on A70-C/C8.

	pH elution		pH elution followed by trypsin treatment		Lewis Y-PAA elution		Lewis Y-PAA elution followed by trypsin treatment		Proteolytic elution	
Round of selection	1	2	1	2	1	2	1	2	1	2
Total number of Colonies	$2x10^6$	$6x10^5$	$6x10^5$	$9.4x10^4$	$6x10^4$	$2.5x10^3$	$1.3x10^3$	$1.2x10^3$	$2.6x10^3$	$2.7x10^4$
Number of binders										
Anti-idiotypic scFv	5	1	0	1	0	2	3	28	9	1
Isotype binders[a]	1	0	0	1	0	0	0	1	0	0
Shared antibody epitope binders[b]	33	15	29	35	25	16	33	24	28	49
Non-specific binders[c]	2	3	3	0	3	5	1	1	1	0
Non-binders[d]	55	77	64	59	68	73	59	42	58	46

[a] scFv-phage, which also binds to an antibody of the same isotype as Ab1
[b] scFv-phage binding to all wells containing any antibody
[c] scFv-phage binding to plastic or blocking agent
[d] scFv-phage not binding. For further explanations see Materials and Methods.

The other elution methods did not yield an increase in anti-idiotypic scFv during the second round. The proteolytic elution resulted in enrichment of scFv recognising shared antibody epitopes concomitantly with a decrease in anti-idiotypic scFv, which can be explained by the prominence of the Ig epitopes on the mAb and the capture antibody on the beads. The non-specific elution gave a slight increase in scFv against shared antibody epitopes when combined with trypsin treatment but a decrease when used alone. Non-specific elution, the method traditionally used, even led to a decrease in the total number of binders after two rounds, which was not the case for other elution methods.

The combination of antigen specific elution with subsequent trypsin treatment of the eluted phage was further evaluated for the generation of large diversities of anti-idiotypic scFv against the other antibodies of different specificities A70-B/B10, PankoMab, and A78-G/A7. Table 9 shows that these selections were even more successful, resulting in 74% to 100% anti-idiotypic scFv phage obtained. Three different naïve phagemid scFv libraries were used and resulted in comparably high percentages of anti-idiotypic scFv. Isotype binders were comparably rare with 26% to 0%. No differences were observed between using immunotubes or magnetic beads for the selection apart from the necessity for much larger amounts of idiotype (Ab1) required as antigen in case of immunotube selections. In addition, the antibody needs prior purification when used with immunotubes whilst magnetic beads work with Ab supernatants.

Table 9: Yield and diversity obtained of anti-idiotypic scFv-phage in seven experiments employing specific elution followed by trypsin treatment.

Antigen experiment	A70-C/C8	A70-B/B10	PankoMab I	PankoMab II	A78-G/A7 I	A78-G/A7 II	A78-G/A7
Elutant	Lewis Y-PAA [100µg/ml]	Lewis Y-PAA [100µg/ml]	Muc1-Tn glyco-peptide [50µg/ml]		a-GP [100µg/ml]		a-GP [100µg/ml]
Rounds of selection	2	2	2	3	3	3	2
Selection on	Beads	Beads	Tubes	Beads	Tubes	Beads	Tubes
Library	Tom J	Tom I+J	Tom I+J	Tom I+J	Griffin.1	Tom I+J	Griffin.1
A. Number of binders							
Anti-idiotypic antibody	28	81	71	73	18	88	65
Isotype binders [a]	1	0	25	15	0	8	n.d.
Non-specific binders [c]	1	0	0	0	0	0	0
Non-binders [d]	42	15	0	6	0	0	36
B. Diversity							
No. of sequenced clones	28	30	17	27	11	10	n.d.
No. of different sequences	16	5	11	21	6	9	n.d.
Diversity in %	57	16	65	78	55	90	n.d.

[a] scFv-phage, which also binds to an antibody of the same isotype as Ab1
[c] scFv-phage binding to plastic or blocking agent
[d] scFv-phage not binding. For further explanations see Materials and Methods. Ab1 A70-C/C8

Sequencing of some of the selected phagemids from the various selections revealed that a broad variety of anti-idiotypic scFv were isolated using the specific elution combined with tryptic cleavage (Table 9). Thereby the diversity is similar after two or three rounds of selection. As an example, from 28 sequenced anti-idiotypic antibodies from the selection on A70-C/C8, 16 different sequences were obtained (57% diversity) (the anti-idiotypic antibodies from the A70-C7C8 and A46-B/B10 selection are further decribed in chapter 2.11.2). Comparably, 44 sequenced anti-idiotypic scFv from the selection on antibody PankoMab, showed 31 different sequences (70%). In another case, out of 21 scFv from the A78-G/A7 selection, 15 proved to be different. An exception to the high diversity obtained in these experiments was the selection on A46-B/B10. Two rounds of selection were made and after the first round only 80 colonies were obtained. Testing after the second round showed that 84% of the clones were anti-idiotypic binders. Of these 81 scFv-phage 30 were sequenced; five of these were found to be different. This gives a diversity of only 16% which is not comparable to the diversities obtained from the other selections due to the limited amount of colonies harvested and used as basis for the second round selection.

Anti-idiotypic scFv candidates identified by ELISA screening were further examined to meet the inhibition criteria for anti-idiotypic antibodies. Therefore, they were tested as scFv-phage for their potential to inhibit the binding of the idiotype to its antigen using ELISA experiments for all antibodies on their respective antigen as well as immunocytochemistry for the A78-G/A7 antibody.

In the ELISA format generally more than 95% of the candidates proved to be anti-idiotypic as shown in Figure 32 with selected scFv. An anti-idiotypic scFv from a different experiment served as the control (B1 in Figure 32 A and A1 in Figure 32 B). As expected, the inhibitory potency varied among the anti-idiotypic scFv. Less than 5% showed no inhibition potential. The inhibition potential of the anti-idiotypic antibodies selected on A70-C/C8 and A46-B/B10 is further examined in chapter 2.11.2.

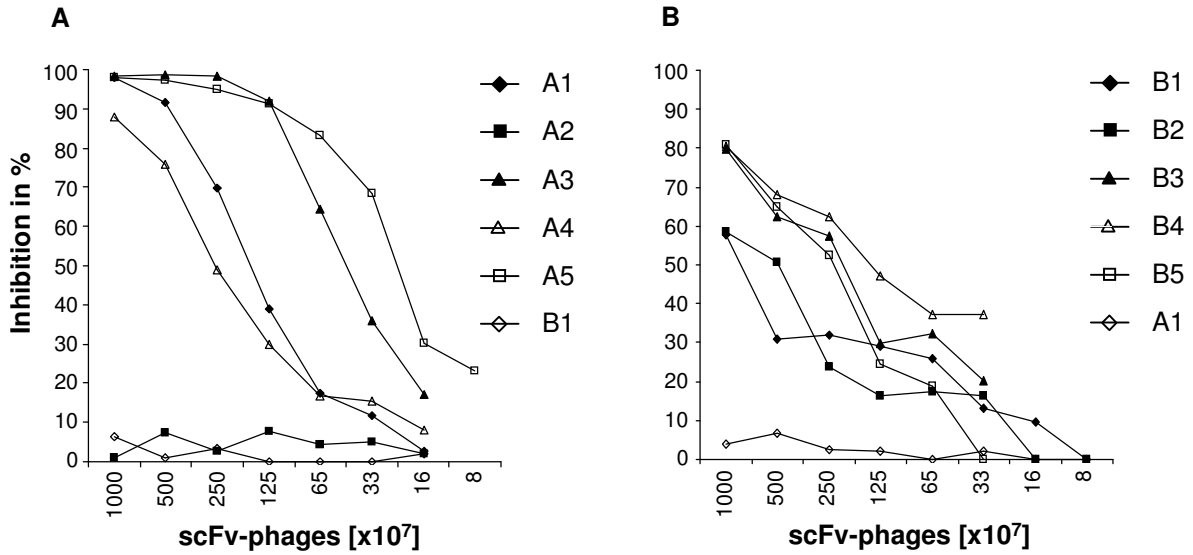

Figure 32: Inhibition analysis of: (A) antibody A78-G/A7 binding to TF on A-GP or (B) antibody PankoMab binding to synthetic, PDTR-glycosylated MUC1 glycopeptide by anti-idiotypic scFv on phage. Various amounts of scFv-phage were preincubated with antibody supernatants and subsequently incubated with their respective antigen. The indicated phage numbers correspond to the number of phage carrying scFv. In addition, there are 100 fold more phage without scFv in the incubation due to the phagemid format. A-clones originate from selections with A78-G/A7 and B-clones from PankoMab selections.

Various anti-idiotypic scFv from the A78-G/A7 selection were tested as scFv-phage for their potential to inhibit the binding of A78-G/A7 to the TF-antigen in its natural environment on the cell surface of a TF-antigen positive KG-1 sub line. As an example, it is shown in Figure 33 A that the TF-anti-idiotypic scFv A5 inhibited the binding completely, while the anti-idiotypic scFv B1, not mimicking the TF-antigen, did not (Figure 33 B). Conversely, B1 and other anti-idiotypic scFv for MUC1 did inhibit the binding of PankoMab to T47D cells, while in this case A5 served as a negative control (data not shown).

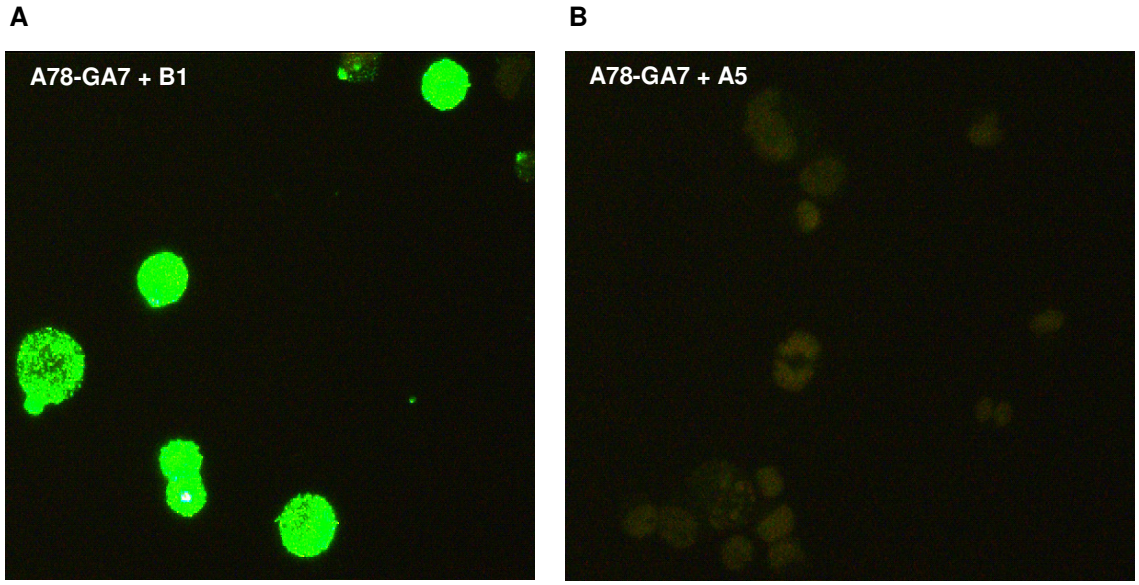

Figure 33: Inhibition of TF-specific binding of antibody A78-G/A7 to KG-1 cells by anti-idiotypic scFv on phage. The antibody A78-G/A7 was preincubated with: (A) TF-anti-idiotypic A5 or (B) MUC1-anti-idiotypic B1 scFv-phage as a control, respectively, and transferred to KG-1 cells. A78-G/A7 was detected by FITC-labelled goat anti-mouse polyclonal antibodies

2.11.2 Anti-idiotypic antibodies mimicking Lewis Y or H type 2

The anti-idiotypic selections, using different elution methods, on A70-C/C8 gave rise to a total number of 50 clones, when clones from the first and second round both were included (Table 8). Independently of the elution method 40 clones were sequenced and 27 different sequences were identified which is 68% in total. Surprisingly, it was found that of these 40 different clones only two clones were found to contain the full length scFv gene, both clones comes from the Lewis Y-PAA elution followed by trypsin treatment. Furthermore, these two clones had the same sequence and all the remaining clones (38, with 26 different sequences) contained a recombined scFv gene. The DNA from all clones was found to be recombined at the same position in the middle of the heavy chain CDR 3. Remaining was only the last bit of the heavy chain CDR 3, the framework region 4, the linker region, and a complete light chain. Phage containing this DNA will therefore only display the VL, the linker, and 16 residues from the heavy chain C-terminus. This gave rise to the name recombined single domain phage (RSD-phage).

Comparison of the reactivity of four of the anti-idiotypic scFv-phage selected on A46-B/B10 (PACA clones) with one scFv-phage and five RSD-phage selected on A70-C/C8 (PACB clones) to their respective antigens showed that the four full length clones from the A46-B/B10 selection and the one full length clone from the A70-C/C8 selection (PACB04) give rise to bigger signals than the RSD-phage (Figure 34).

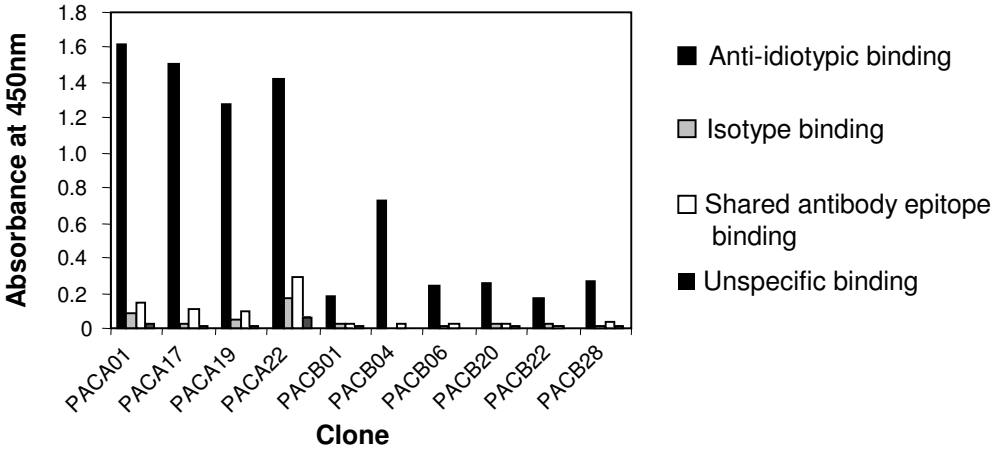

Figure 34: Comparison of anti-idiotypic binding of four PACA clones with six PACB clones of which five are single domains. PACA clones are tested on immobilised anti-mouse IgM incubated with A46-B/B10; PACB clones are tested on A70-C/C8. Phage are added directly from the cell culture supernatant to the ELISA without precipitation or titer determination. Detection is made with mouse anti-M13 POD.

Several titer experiments (on ampicillin resistant plates, which allow only colony formation from bacteria infected with phage containing a fusion encoding phagemid) where performed to estimate the concentration of PACA and PACB phage in cell culture supernatants. As a result both types of clones produced approximately the same amount of phage, which contained fusion protein DNA. The titer determinations on trypsinated phage were generally between three and five times higher for the PACB clones when compared to the PACA clones, which determines the actual amount of phage displaying a wt p3. To support this, precipitated phage were Western-blotted and detected with anti-p3 antibody, to show the difference between the amounts of phage p3 with and without fusion protein (Figure 35 A). As seen in Figure 35 A, the display level of both the RSD-phage and scFv-phage from the A70-C/C8 selections is higher than phage originating from the A46-B/B10 selections.

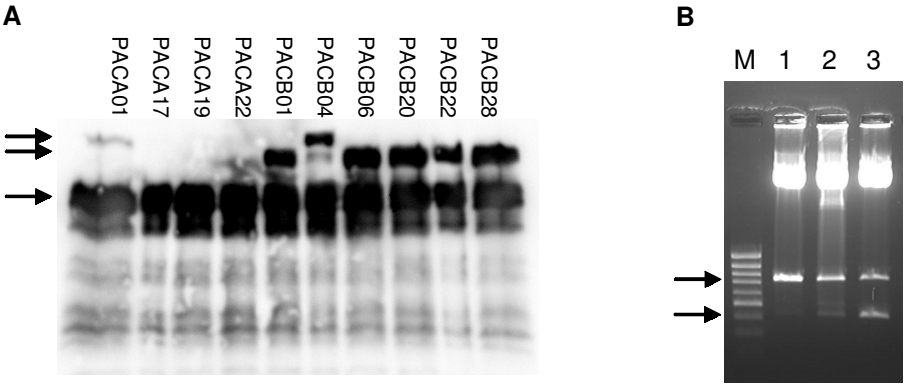

Figure 35: (A) Western blot of a 10% SDS-PAGE loaded with equal amounts of protein (determined by absorbance measurements at 280nm) from twice precipitated phage preparations. The three arrows indicate the positions of scFv-protein 3 fusion (top), RSD-protein 3 fusion (middle), and p3 (bottom), respectively. (B) A 1.5% agarose gel with EtBr loaded with 100bp marker (lane M), 10µg of a plasmid preparation cut with NcoI and NotI from (lane 1) the Tom J library, (lane 2) the total rescue 1. round selection, and (lane 3) total rescue 2. round selection. The two arrows indicate the sizes of the DNA cut out of the plasmids and correspond to a full scFv (top) and a recombined single domain DNA (bottom), respectively.

Only the PACA01 gave rise to a slightly visual band whereas the PACB clones all clearly contained fusion protein. Several additional blots were made with samples having the same phage titer (determined of ampicillin resistant plates). These blots showed the presence of much higher amounts of p3 without fusion protein in the PACA clones than in the PACB clones. p3 without fusion protein is encoded by the helperphage genome which contains a kanamycin resistance gene and was therefore not seen in the titer determination on ampicillin plates. The PACB clones and especially the RSD-clones display more fusion protein than the PACA clones. This indicates that the reduced binding of the RSD-phage is not caused by a lower amount of fusion protein displaying phage.

To show that the RSD-phage are not an artefact generated in one of the selection rounds in the specific elution followed by trypsin treatment midi preps were made from overnight cultures of the Tom J bacteria library stock, the total rescue of bacteria after the 1. round, and 2. round selections. 10µg of the midi preps were cut with NotI and NcoI and loaded on a 1.5% agarose gel (Figure 35 B). This showed RSD DNA is clearly enriched during the selection. Furthermore, several measurements of the doubling times of bacteria containing a PACA or a PACB phagemid showed that there is no difference in growth rate. The clones are therefore not selected due to growth advantages.

Competition experiments performed on immobilised Lewis Y-PAA where the PACB phage are added in solution to inhibit the binding of A70-C/C8 to Lewis Y where performed. They showed that none of the RSD-phage were able to inhibit A70-C/C8 binding to Lewis Y. Only the full length scFv PACB04 clone was able to inhibit the binding slightly (data not shown). The results of the PACB clone investigation indicate that these clones are selected because they display more fusion protein or suppress p3 wt incorporation in the phage but they were also found repeatedly to bind to the A70-C/C8.

The five PACA scFv-phage originating from the selection on A46-B/B10 were also tested for inhibition of A46-B/B10 binding to Lewis Y in ELISA (Figure 36). All these clones inhibited the A46-B/B10 binding to Lewis Y in a concentration dependent manner.

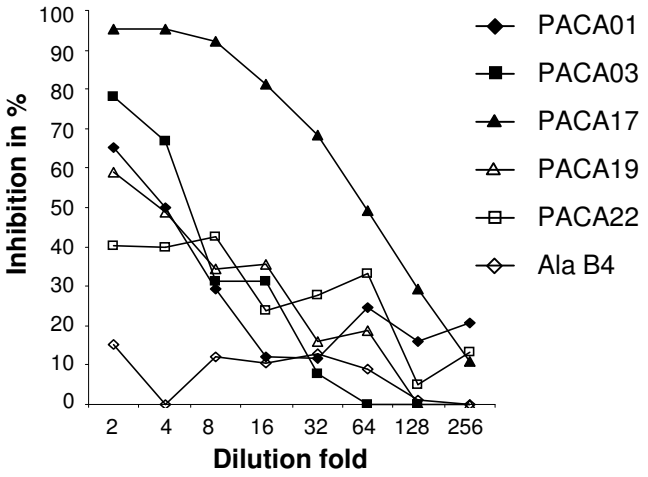

Figure 36: Inhibition analysis of antibody A46-B/B10 binding to Lewis Y-PAA by anti-idiotypic scFv on phage. Dilutions of precipitated and 10 fold concentrated scFv-phage were preincubated with A46-B/B10 supernatant and subsequently incubated on an ELISA plate with coated Lewis Y-Paa. The indicated numbers correspond to the dilution fold of the precipitated and 10 fold concentrated phage solution. PACA clones originate from selections on A46-B/B10 and the negative control Ala B4-clone from PankoMab selections.

The textbook like curve obtained for PACA17 inhibition of A46-B/B10 binding to Lewis Y-PAA coated on microtiter plates (Figure 36) made us investigate the mimicry of this clone closer. The binding of PACA17 to three other Lewis Y recognising antibodies of this thesis (A70-A/A9, A70-C/C8, A51-B/A6 (see chapter 2.1), and additionally to A63-D/B12 (an unpublished antibody, which is similar to A46-B/B10) was tested. Binding was only found to A63-D/B12 (Figure 37), whereas no binding was found to A51-B/A6.

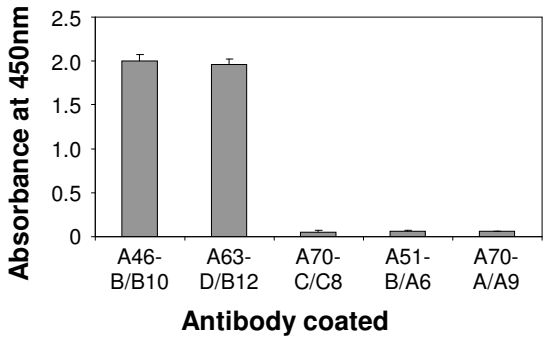

Figure 37: Binding of PACA17 to antibodies recognising Lewis Y. PACA17 scFv was coated, followed by incubation with Lewis Y binding and secondary antibodies. Signals are subtracted background binding to plastic.

2.11.3 Generation of Ab3

The potential of the anti-idiotypic clone PACA17 selected against the monoclonal antibody A46-B/B10 to induce a humoral immune response was investigated by immunising 10-12 weeks old Balb/c female mice with pure scFv protein. Different strategies were investigated. Groups of three mice were immunised with PACA17 scFvs alone, mixed with incomplete Freunds adjuvant (IFA) or fused to the amino-terminal domain I (DI) of phage protein 3 (p3). The amino-terminal DI of p3 was furthermore used for immunisation both alone and in combination with PACA17 scFv to investigate its adjuvant effect. The results are described in chapter 2.12. For preparation the gene for PACA17 was cloned into the pKBJ3 vector which then encodes a scFv fusion to phage protein p3 domain I (Jensen, Larsen et al. 2002). A vector encoding only DI was made by cloning a short oligonucleotide into the pKBJ3 vector. PACA17 and PACA17-DI fusion proteins were purified by metal affinity chromatography and ion-exchange chromatography. DI was purified only by metal affinity chromatography. Yields and purities of expressions and purifications of DI of p3 alone and PACA17 as scFv and in fusion with DI all gave similar results of approximately 2.5mg pure protein per 1 culture. Figure 38 shows an SDS-PAGE analysis of the purity of the proteins. No binding activity increase was observed from the non-fused to the fused PACA17, as was the case for other scFv (Jensen, Larsen et al. 2002). The mice were immunized twice with: L36 (50µg), L36 (50µg)+ Incomplete Freund's Adjuvant (IFA), L36-DI (50µg), PACA17 (50µg), PACA17 (50µg) + IFA, PACA17-DI (75µg), PACA17 + DI (50µg + 25µg), and DI alone (25µg). Injections were given intraperitoneal (i.p.) at Day 0 and Day 14, and blood samples were collected at day –1 and day 28.

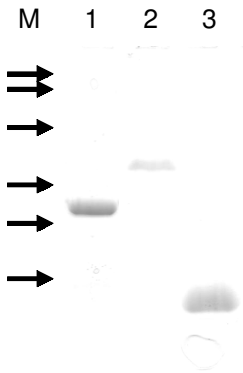

Figure 38: SDS-PAGE of the purified proteins. Lane 1 PACA17, lane 2 PACA17-DI, and lane 3 DI. Lane M is prestained marker and arrows indicate the sizes 113, 93, 53, 35.5, 28.5, and 21kDa.

The sera from mice immunised with the anti-idiotypic scFv PACA17 were in ELISA in triplicates analysed for binding to a small panel of PAA coupled carbohydrates; namely Lewis Y, H type 2, H disaccharide, and fucose. Figure 39 shows that the mice were able to generate a humoral response which recognised Lewis Y related carbohydrates, when immunised with the anti-idiotypic antibody PACA17. Generally the signals from preimmune sera were never higher than those to BSA. Binding against BSA is used as background and subtracted from the signals against the carbohydrates. Strong responses of the IgM isotype against the carbohydrates are seen when PACA17 is used in combination with incomplete Freunds adjuvant (IFA) (mouse B and C) or DI (mouse A and B). The sera from mice immunised with PACA17 and PACA17-DI gave also rise to signals against Lewis Y carbohydrates, but the intensity is lower. The IgM antibodies in the sera do in all but one mouse react with H type 2 (PACA17-DI mouse B). Two mice gave only response against H type 2 (PACA17 + DI mouse C and PACA17-DI mouse C) and three mice give the major response against H type 2 (PACA17 mice A and B and PACA17-DI mouse A). The remaining mice all give higher IgM responses against other carbohydrates than H type 2 but the sera do in all cases also recognise H type 2. Two mice generated IgG antibodies that reacted strongly with carbohydrates (PACA17 + DI mouse A and PACA17-DI mouse C). Three mice showed low or trace reaction of IgG antibodies with carbohydrates (PACA17 mouse B and PACA17-DI mouse A and B). Theses IgG antibodies show no reaction against the H type 2 carbohydrate but show specificity against the H disaccharide or the fucose carbohydrate. The mice immunised with DI alone showed either no or very low response against the carbohydrates and only IgM antibodies were obtained (data not shown).

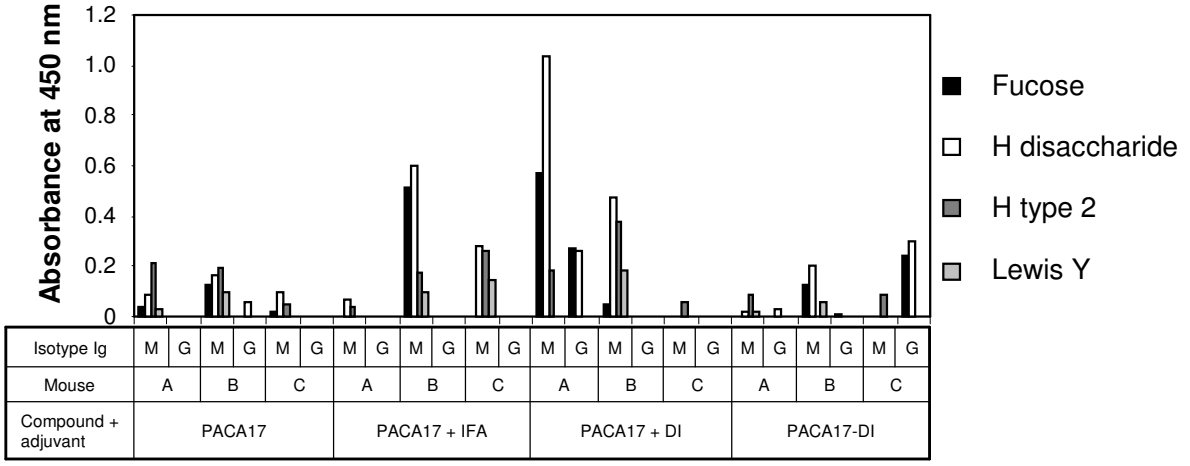

FIGURE 39: Diagram of PACA17 sera specificity. Four different carbohydrates were immobilized in ELISA and sera were subsequently incubated in a 1:30 dilution (diluted with 3% BSA in PBS). Detection was made with anti mouse IgG or IgM antibody POD coupled. In the diagram is for each serum subtracted a background value determined against an uncoated well blocked with 3% BSA in PBS.

2.12 Adjuvant effect of domain I of phage protein 3

Adjuvants are used in combination with the specific antigen to enhance the immunity of the vaccine. Presently aluminium-based mineral salts and oil-based emulsion are the ones used in licensed vaccines (Singh and O'Hagan 1999; Alving 2002). Recombinant protein offer many advantages when used as vaccine such as reduced toxicity. The disadvantage is though that they then often are poorly immunogenic when administered alone. The results described in this section regard a new possible adjuvant.

Previous studies have shown that a fusion of a scFv to the N-terminal domain I (DI) of the filamentous bacteriophage protein 3 (p3) had several different beneficial effects on the in vitro binding activity of the scFv (Jensen, Larsen et al. 2002). We here investigated if the anti-idiotypic scFvs selected by phage display (represented by the clone PACA17 selected against the monoclonal antibody A46-B/B10) would also benefit from this molecular context of selection in immunisation. The sera analysed were obtained from the immunisations described under 2.11.3. By analysing the IgG isotype of these sera in ELISA for binding to PACA17 it was investigated if DI or DI fusions have an enhancing effect on the immune response. We determined the profile of Th1 and Th2 type T cell response via comparison of the antibody isotype response IgG1 vs IgG2a. For supporting the data another scFv (L36), which recognises laminin-1 (Sanz, Kristensen et al. 2001), was included by immunising Balb/c mice with L36, L36 + Incomplete Freunds Adjunvant, and L36-DI using the same protocol as for PACA17.

ELISA data obtained in testing the PACA17 sera, with and without different adjuvants, are shown in Figure 40. The data show that the IgG (IgG1 and IgG2a) responses towards PACA17 scFv are increased by fusion to DI of p3 compared to the scFvs alone. The observed increases were comparable to the response of PACA17 scFv supplemented with IFA. The response against PACA17 scFv supplemented with DI was interestingly higher than the one obtained with PACA17 scFv supplemented with IFA and PACA17-DI fusion. One of the mice (PACA17 + IFA mouse C) immunised with PACA17 supplemented with IFA failed to produce

an IgG response, whereas all the mice including the DI in the vaccine showed IgG responses. The sera from mice immunised with DI alone did not give rise to any antibodies recognising the PACA17 in ELISA in the used dilution.

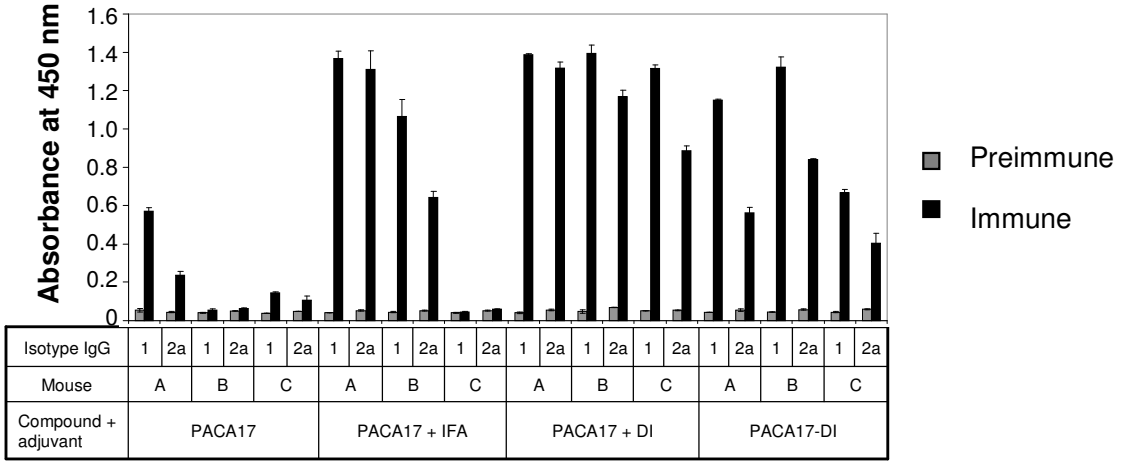

FIGURE 40: The bar diagram shows the immune response for different mice immunised with PACA17 scFv with and without different adjuvants. The immune response was for each mouse determined specifically against the non-fused scFv PACA17. The immune responses were analysed for their IgG1 and IgG2a subclass distribution. The error bars represent the standard deviation. Sera dilution is 1:1000. Abbreviation: DI, domain I of p3.

Figure 41 shows in a similar way the ELISA data obtained with sera from the immunisations with L36 with and without different adjuvants. Here again the fusion of L36 to DI gave rise to an increase in IgG responses but in the L36 case the observed increases were slightly lower than the L36 scFv supplemented with IFA. Also in the case of L36 supplemented with IFA one mouse failed to produce an IgG response (L36 + IFA mouse C).

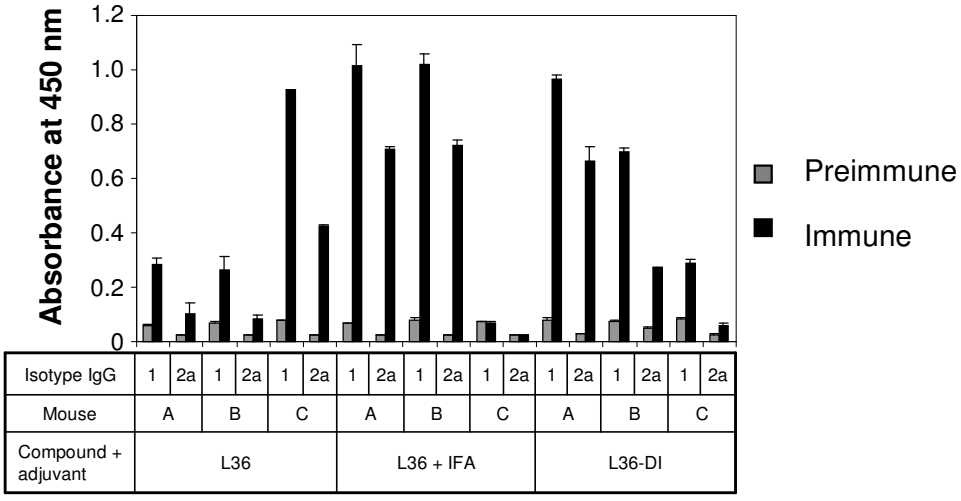

FIGURE 41: The bar diagram shows the immune response for different mice immunised with L36 scFv with and without different adjuvants. The immune response was for each mouse determined specifically against the non-fused scFv L36. The immune responses were analysed for their IgG1 and IgG2a subclass distribution. The error bars represent the standard deviation. Sera dilution is 1:1000. Abbreviation: DI, domain I.

In general for both antibodies, the subclass distribution of IgG1 and IgG2a shows higher IgG1 levels than IgG2a, although both subclasses were prominent as determined by the observed ELISA signals. Despite that the two IgG subclasses are detected with two different antibodies**,** the ELISA signals are comparable, since the two antibodies show equivalent activity on the same amount of IgG1 and IgG2a, respectively.

To sum up the results an adjuvant property of the N-terminal fragment of p3 was found, as the immunisations with non-immunogenic scFvs fused to the N-terminal domain of p3 induceed an immune response towards the scFv.